Supporting Information

By employing racemization strategies to simultaneously enhance the quantum yield, lifetime, and water stability of room-temperature phosphorescent materials

Zenggang Lin[a], Peng Zhang[a, b], Fuqiang Song[a], Yuzhu Yang[a], Xuan Miao[a] and Weisheng Liu[a*]

Experimental Procedures

Reagents and materials

The following reagents used in the experiments were purchased from Aladdin Chemical Reagents Network unless otherwise stated. Polyacrylonitrile (PAN, molecular weight (Mw) = 150,000 g/mol), poly (methyl methacrylate) (PMMA, molecular weight (Mw) = 120,000 g/mol), and polystyrene (PS, molecular weight (Mw) = 100,000 g/mol) were purchased from sigma-Aldrich. ^{1}H and ^{13}C NMR spectra were recorded on a Bruker AVANCE III 400 spectrometer with $CDCl_3$ as solvent. XRD was recorded using a Rigaku D/Max-2400 X-ray diffractometer. Scanning electron microscope (SEM) image of the three films were measured on FEI Quanta 400 FEG America FEI. UV-Vis absorption spectra were measured by a Perkin Elmer Lambda 950^{+}Refle instrument. Fluorescence spectra were recorded using a Hitachi F-7000 spectrophotometer. Phosphorescence spectra were measured by FLS 920 Lifetime Spectrometer and Steady State Spectrometer. Photoluminescence quantum efficiency was obtained on Edinburgh FLS 1000 fluorescence spectrophotometer equipped with an integrating sphere. The Φ_{Phos} measurement was conducted using a microsecond lamp as the excitation source, and the fluorescence section can be filtered out by using the gating delay system, so that more accurate Φ_{Phos} was obtained. The quantum yield measurements on FLS 1000 were auto-calculated mainly based on different phosphorescence emission spectra of reference and samples, and ΦPhos was calculated by FLS 1000 software. Single crystal data were collected on a Bruker Smart APEXII CCD diffractometer using graphite monochromatic Mo Kα radiation (λ = 0.71073 Å) or Cu Kα radiation (λ = 1.54184 Å). The photos were taken with an iPhone 13 cell phone.

Theoretical calculation

The structure of rac-NDBD-Ph, R-NDBD-Ph, R-NDBD-Ph-acid and R-NDBD-Ph-base was optimized with dispersion-corrected density functional theory (DFT-D3) at the PBE1PBE/def2-SVP level, and SOC of three phosphors and PAN matrix, the energy of S_n and T_n was calculated at PBE1PBE/def2-TZVP with the time-dependent density functional theory (TD-DFT) method using the ORCA program package.[1] Complexation energy was estimated using the PBE1PBE/def2-TZVP approach including the Grimme's empirical dispersion correction with Becke-Johnson damping (GD3BJ), zero-point energy (ZPE) and BSSE correction: Ecomp = $E_{complex}$ - E_{PAN} - $E_{phosphors}$.[2,3]The electrostatic potential (ESP) values were calculated by Multiwfn program package[4] and ESP pictures were obtained from VMD program package.[5]

Synthesis of chiral compounds

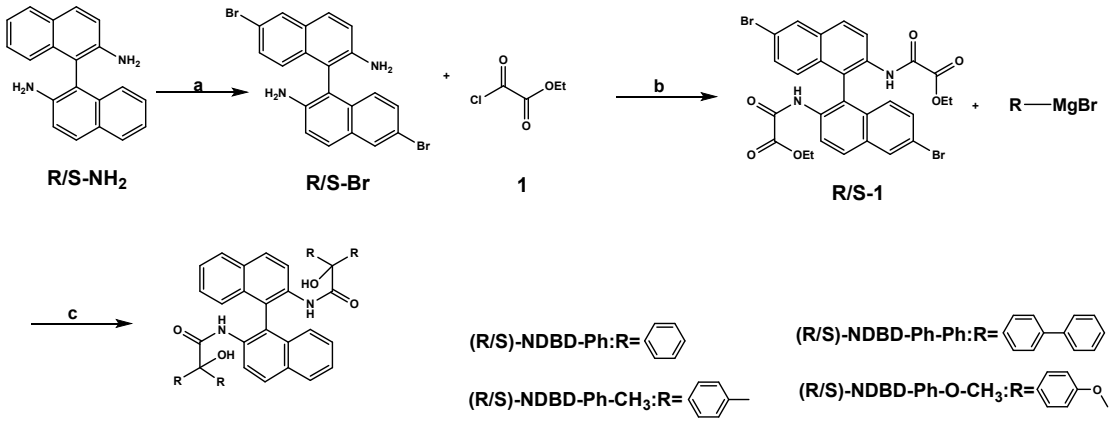

Scheme S1. Synthetic route of R/S-NDBD.

a: To a round-bottomed flask, R/S-NH_2 (2 mmol, 0.57 g), $TBABr_3$ (4.2 mmol, 2.03 g), $CaCO_3$ (4.2 mmol, 0.42 g), and CH_2Cl_2 (20 mL) were added sequentially, the reaction was carried out for 20 min under Ar atmosphere at 0 °C, and then the reaction was continued for 1.5 h after the mixture was brought up to the ambient temperature. At the end of the reaction, the reaction was quenched by adding saturated NH_4Cl solution to the reaction system, and then extracted with CH_2Cl_2, the organic phase was washed with brine, dried and concentrated, and the brown target product R/S-Br (0.75 g, yield = 85%) was isolated by column chromatography.

b: To a round-bottomed flask, R/S-Br (1 mmol, 0.44 g), $NaHCO_3$ (5 mmol, 0.42 g) and CH_2Cl_2 (5 mL) were added sequentially, and 1 (2.4 mmol, 0.27 mL) was added dropwise under an Ar atmosphere at 0°C. After completion of the dropwise addition, the mixture was brought up to the ambient temperature, and the reaction was carried out for 12 h. At the end of the reaction, saturated

NH_4Cl solution was added to the reaction system to quench the reaction. At the end of the reaction, the reaction was quenched by adding saturated NH_4Cl solution to the reaction system, then extracted with ethyl acetate, the organic phase was washed with brine, dried and concentrated, and the white target product R/S-1 (0.75 g, yield = 85%) was isolated by column chromatography.

c: R/S-1 (1 mmol, 0.64 g) and THF (5 mL) were added to a round-bottomed flask, and R-MgBr (1M, 10 mL, 10 mmol) dissolved in THF was added dropwise under Ar atmosphere at 0°C. After completion of the dropwise addition, the mixture was brought up to the ambient temperature and the reaction was carried out for 12 h. At the end of the reaction, the reaction was quenched by addition of saturated NH_4Cl to the reaction system, and the product was extracted with ethyl acetate. The reaction was extracted with ethyl acetate, and the organic phase was washed with brine, dried and concentrated, and the white target product R/S-NDBD was isolated by column chromatography. **R-NDBD-Ph:** white solid，yeild 75%。**S-NDBD-Ph:** white solid，yeild 82%。

R-NDBD-Ph-Ph: white solid，yeild 46%。**S-NDBD-Ph-Ph:** white solid，yeild 55%。

R-NDBD-CH_3: light yellow solid，yeild 90%。**S-NDBD-CH_3:** light yellow solid，yeild 93%。

R-NDBD-O-CH_3: solid earth color，yeild 72%。**S-NDBD-O-CH_3:** Solid earth color，yeild 86%。

Purification method

Chiral organic phosphors were purified three times by column chromatography. Racemic compounds were obtained by mixing at a stoichiometric ratio of 1:1. The polymer PAN was purchased from Aladdin (Mw = 150000), and the purification procedure was as follows: after the PAN powder was completely dissolved in the solvent DMF, the solvent ethanol was dropped into the DMF solution to precipitate the PAN, which was collected by filtration. The process was repeated three times and the collected PAN powder was dried in a vacuum oven.

Preparation of doped films

A mixture of organic phosphors ((R/S/rac)-NDBD-Ph, (R/S/rac)-NDBD-Ph-Ph, (R/S/rac)-NDBD-CH_3, and (R/S/rac)- NDBD-O-CH_3)/PAN/DMF (1.25 mg / 50 mg / 1 mL of DMF) was heated and stirred until transparent, and the mixture was cast on a quartz substrate and then annealed at 110 °C for 1 h to prepare the film.

Single crystal synthesis

The single crystals obtained in this paper were all synthesized by solvent volatilization method. [CCDC 2336502, 2336503, 2336504 and 2336505] contains supplementary crystallographic data for this paper. The data is available free of charge through www.ccdc.cam.ac.uk/data_request/cif from the Cambridge Crystal data Center.

Table S1. Photophysical parameters for the doped rac-NDBD-Ph@PAN, R-NDBD-Ph@PAN and S-NDBD-Ph@PAN films.

Sample	Fluo.			Phos.		
	λ_{em} [nm]	Φ_F [%]	τ [ns]	λ_{em} [nm]	Φ_P [%]	τ [ms]
rac-NDBD-Ph@PAN	293,392	12.6	2.13,19.63	514,543	1.54	954,1357
R-NDBD-Ph@PAN	293,392	7.6	1.54,17.52	514,543	0.92	759,1068
S-NDBD-Ph@PAN	384,396	7.8	1.72,18.16	514,543	0.96	813,1159

Table S2. Photovoltaic parameters of the doped rac-NDBD-Ph@PAN films are compared with previous literature.

Sample	Fluo.		Phos.		Ref.
	Φ_F [%]	τ [ns]	Φ_P [%]	τ [ms]	
DBT@PVA	/	1.23,9.12	1.51	116.42,109.30	6
PMA/LDH@PAA	/	3.13	8.7	170	7
TBB-6OMe@PAN	2.34	2.7	0.61	968.1	8
4AIN@PMMA	11.28	2.338	6.01	1077.5,1076.7	9
DPCz@PVA	19.05	7.47	0.81	2044.86	10
rac-NDBD-Ph@PAN	12.6	2.13,19.63	1.54	954,1357	**This work**

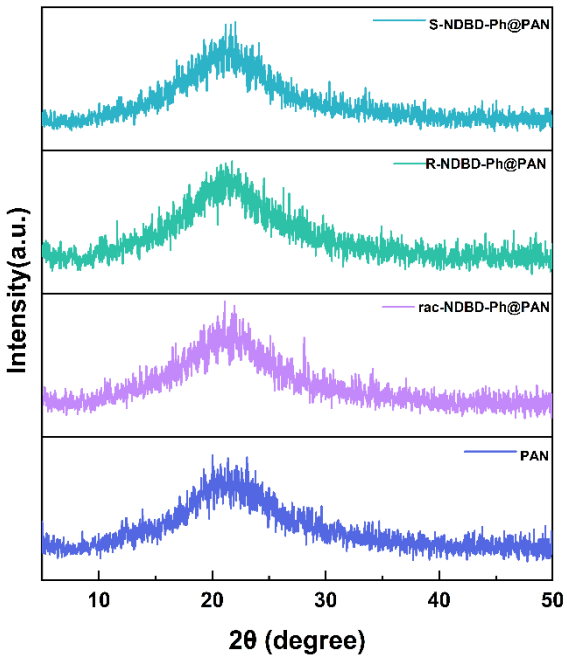

Figure S1. XRD patterns of PAN and doped films.

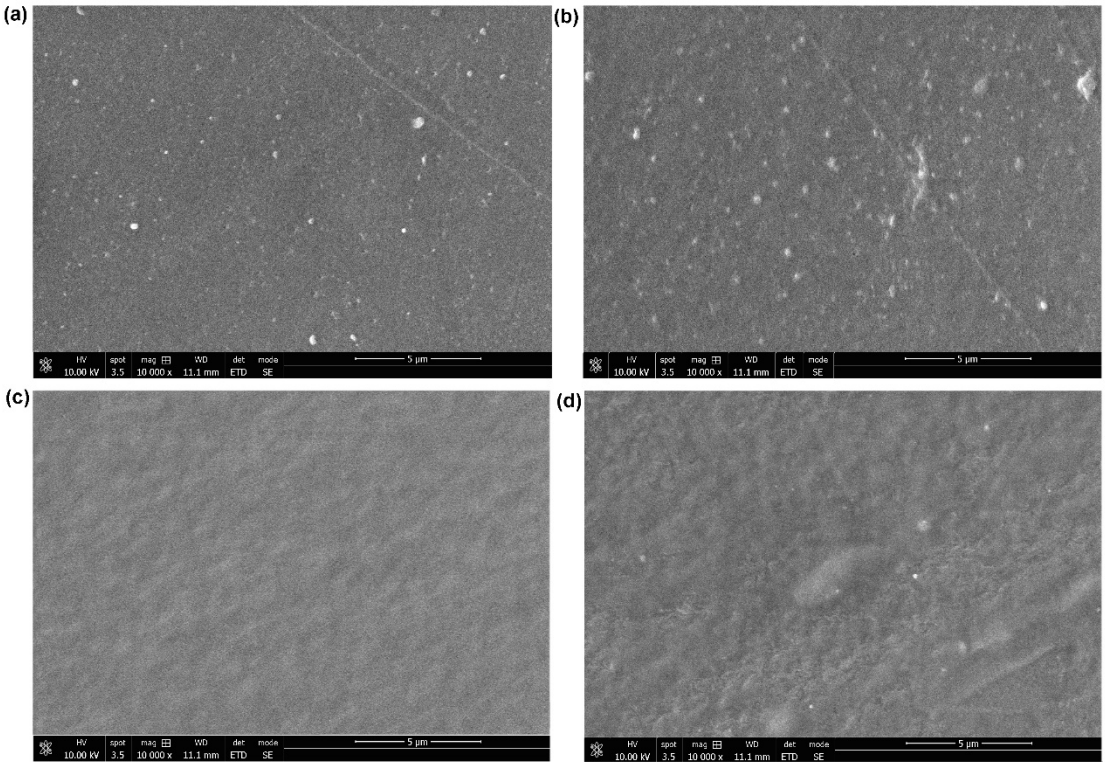

Figure S2. SEM images of doped films (a) R-NDBD-Ph@PAN, (b) S-NDBD-Ph@PAN, (c) rac-NDBD-Ph@PAN (2.5% doping ratio) and (d) rac-NDBD-Ph@PAN (5% doping ratio).

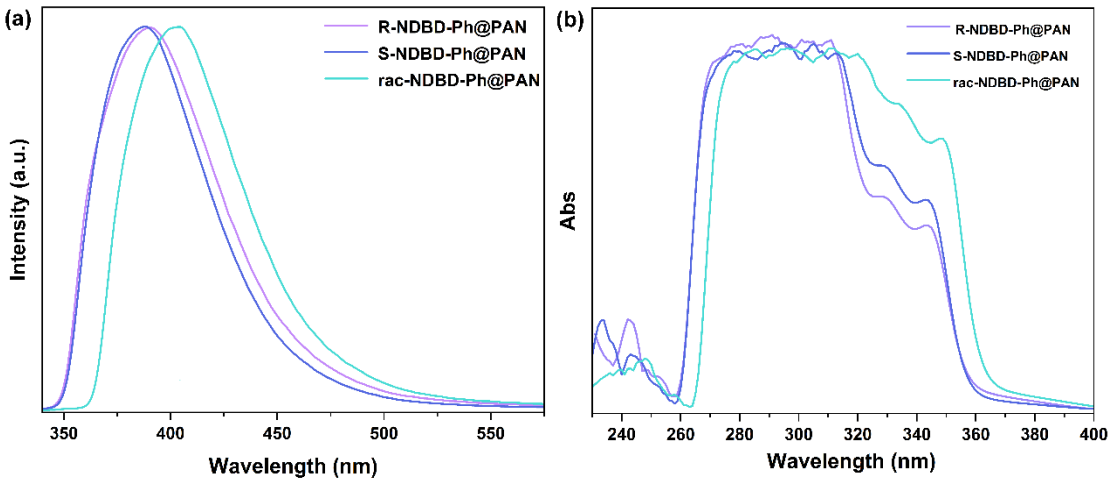

Figure S3. (a) Fluorescence emission spectra and (b) UV absorption spectra of doped films R-NDBD-Ph@PAN, S-NDBD-Ph@PAN and rac-NDBD-Ph@PAN in solution state. The solution was prepared at a concentration of (R/S/rac)- NDBD-Ph/PAN/DMF (2.5 mg / 100 mg / 2 mL).

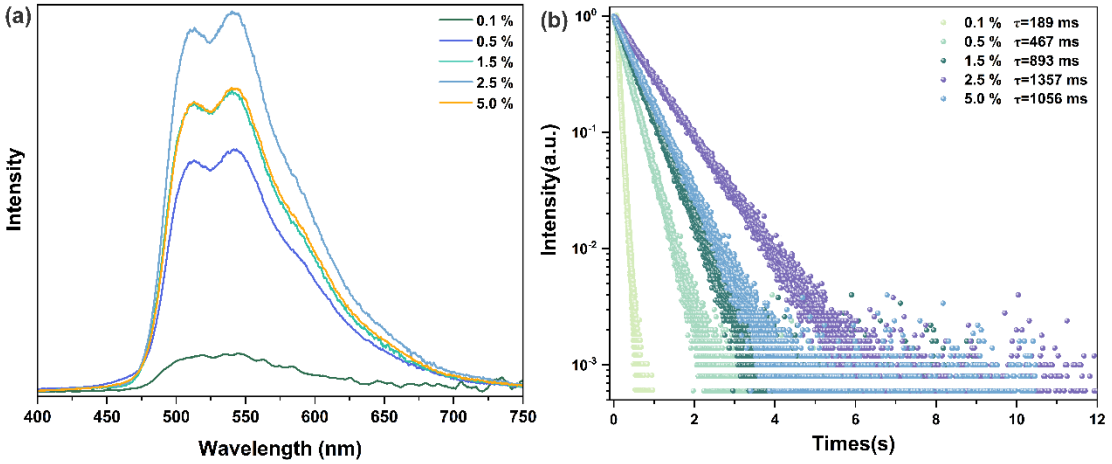

Figure S4. Photophysical properties of doped films with different doping ratios. (a) Phosphorescence spectra and (b) time-resolved phosphorescent decay curves at 543 nm of doped films rac-NDBD-Ph@PAN at different doping concentrations.

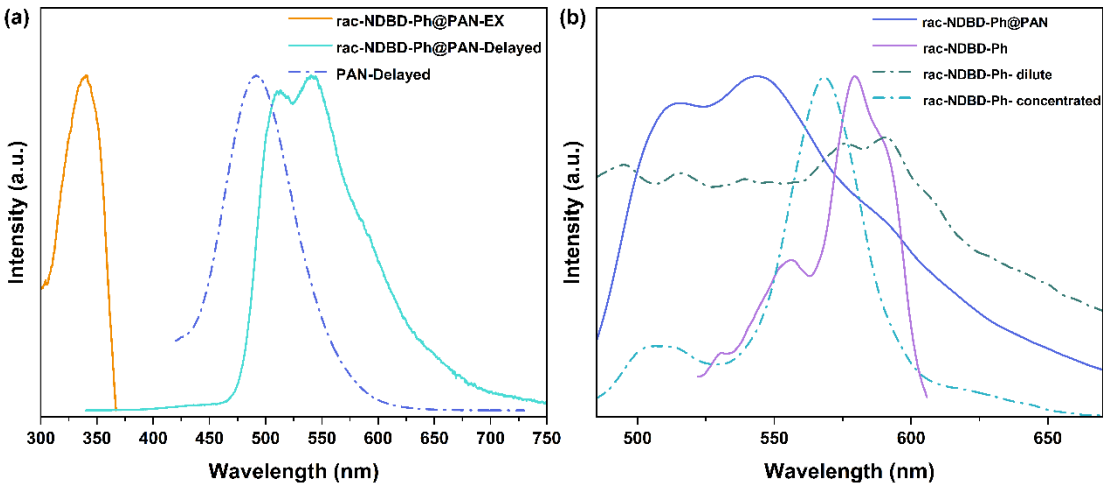

Figure S5. (a) Overlapped phosphorescent emission spectra of pure PAN film and the excitation emission spectra as well as the phosphorescence emission spectra of the doped film (delay time: 2 ms). (b) Overlapped phosphorescence emission spectra of doped films and organic phosphors measured in solution and powder state, respectively (delay time: 2 ms).

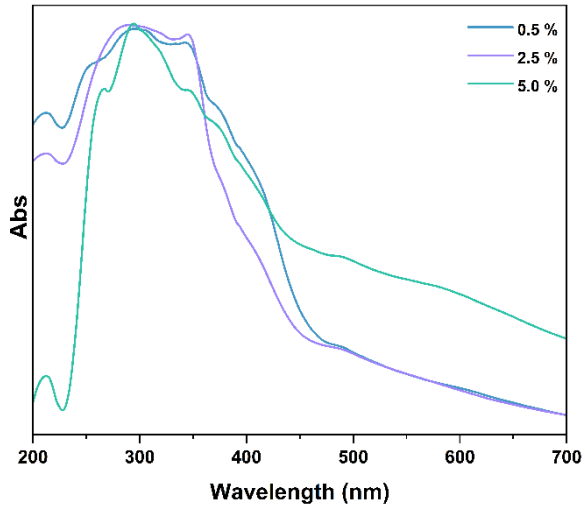

Figure S6. UV absorption spectra of doped films with organic phosphors doped at different doping concentrations.

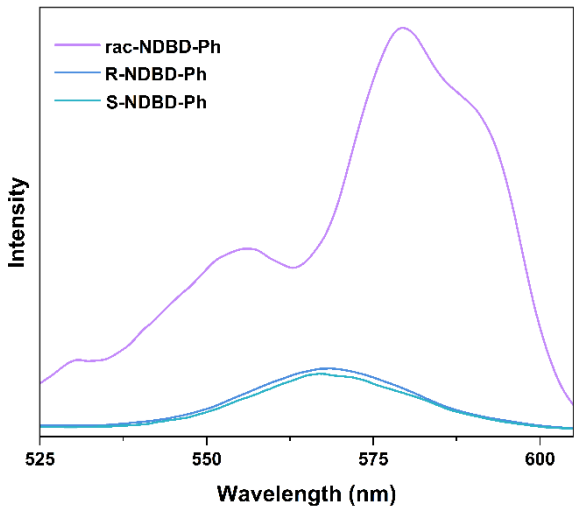

Figure S7. The phosphorescence emission spectra of rac-NDBD-Ph and R/S-NDBD-Ph in single crystals.

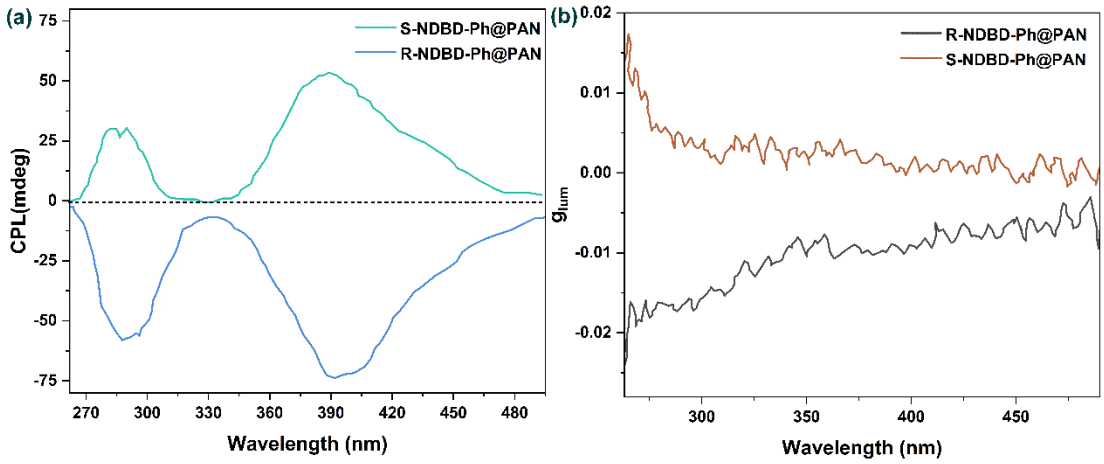

Figure S8. Circularly polarized luminescence properties of doped films S-NDBD-ph@PAN and R-NDBD-ph@PAN. (a) S-NDBD-ph@PAN and R-NDBD-ph@PAN displayed subtle differences in the spectral shapes of the CPL signals (particularly, at extreme wavelengths around 390 nm. (b) R-NDBD-ph@PAN and S-NDBD-ph@PAN doped films with $|gem| \approx 1.72 \times 10^{-3}$ are almost mirror images of each other.

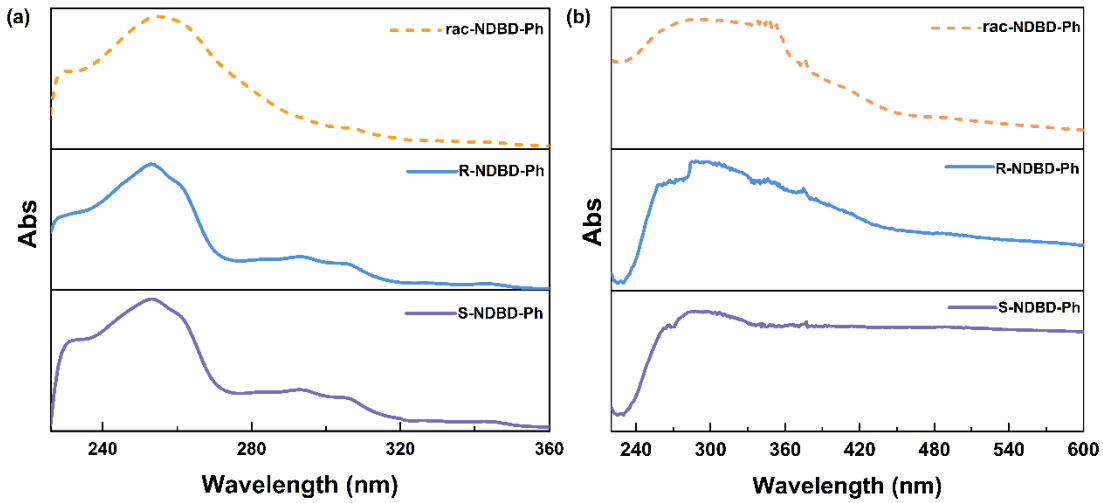

Figure S9. Absorption spectra of organic phosphors (a) in dichloromethane solution and (b) solid state.

Table S3. Structure data of rac-NDBD-Ph and R-NDBD-Ph single crystals.

Name	rac-NDBD-Ph	R-NDBD-Ph
Formula	$C_{48}H_{34}Br_2N_2O_4$	$C_{51}H_{42}Br_2N_2O_7$
Temperature/K	149.98(14)	297.74(18)
Crystal system	monoclinic	monoclinic
Space group	P2_1n	$C2_y$
Cell Lengths (Å)	a=12.1612(2)	a=36.1548(8)
	b=10.2907(2)	b=10.7003(2)
	c=36.8655(7)	c=12.0413(2)
Cell Angles (°)	α= 90	α= 90
	β= 96.834(2)	β= 97.414(2)
	γ= 90	γ= 90
Cell Volume (Å^3)	4580.84(15)	4619.44(16)
Z	4	4
Density (g/cm^3)	1.251	1.373
F (000)	1752	1952
Crystal size (mm^3)	0.14 × 0.12 × 0.04	0.14 ×0.13×0.12
Radiation	CuKα (λ = 1.54184)	Cu Kα (λ = 1.54184)

CCDC number	2336502	2336503

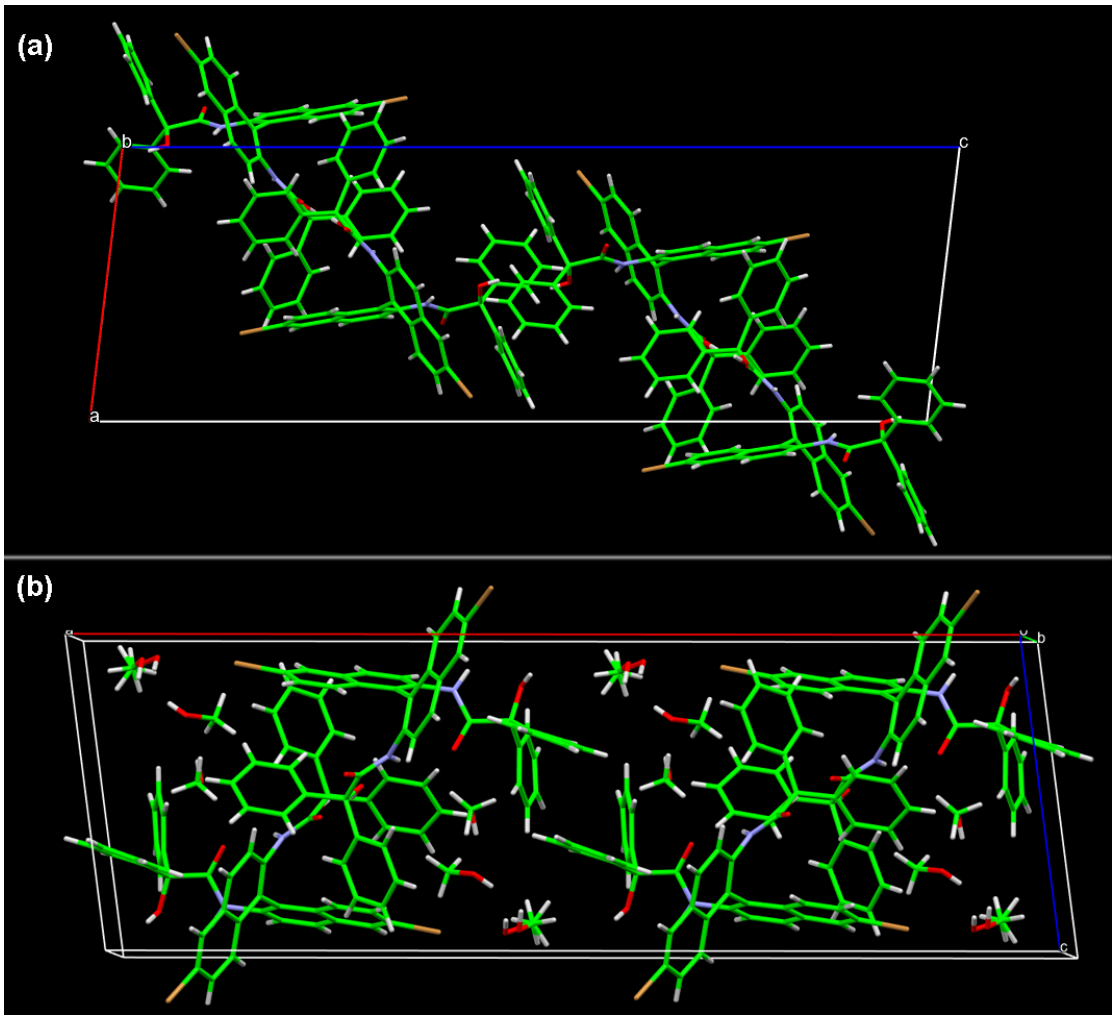

Figure S10. Molecular packing of NDBD-Ph in different configurations from (a) rac-NDBD-Ph and (b) R- NDBD-Ph in a crystal unit cell.

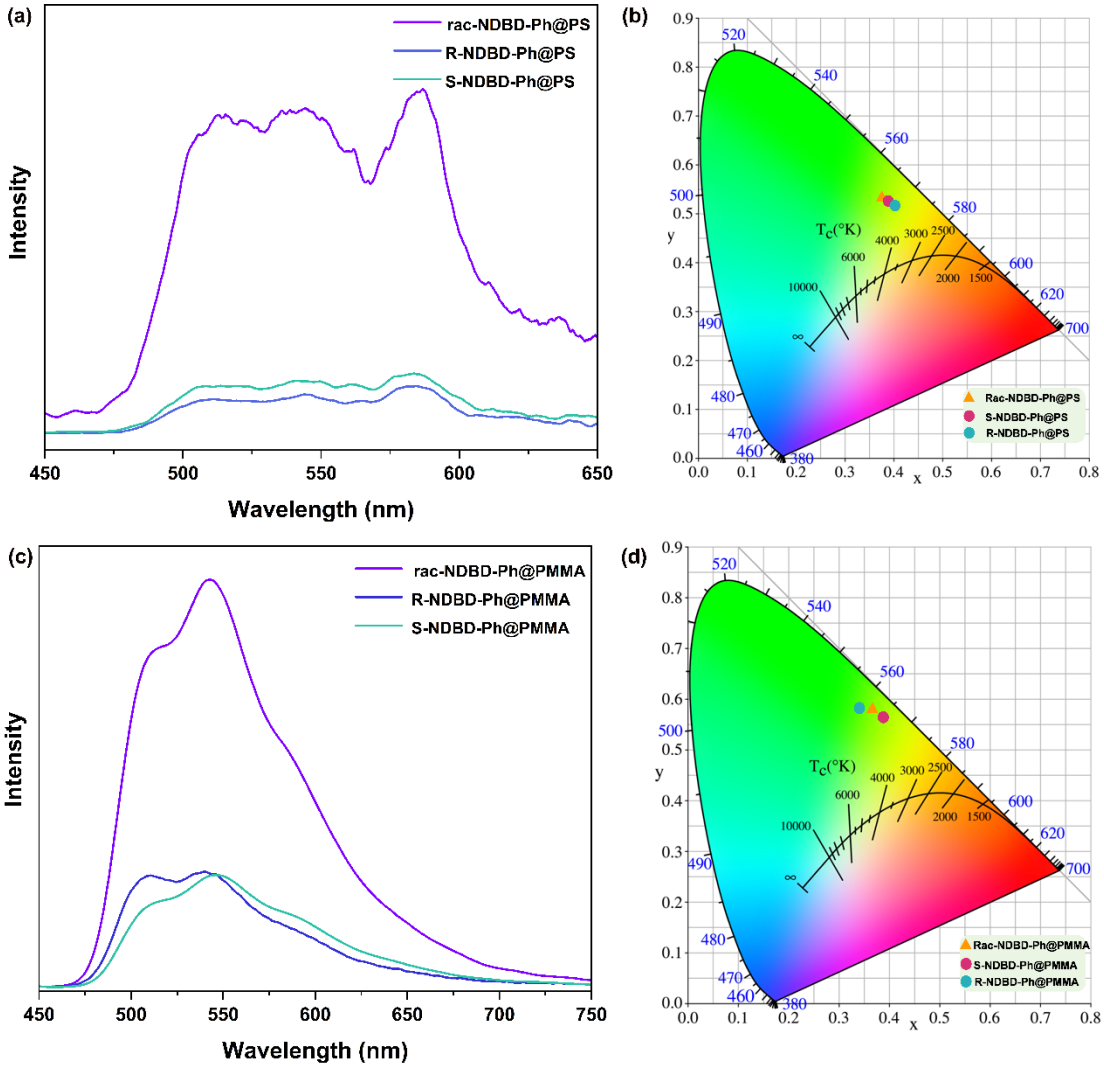

Figure S11. (a, c) Phosphorescence spectra and (b, d) the CIE 1931 coordinates of organic phosphors rac-NDBD-Ph and R/S-NDBD-Ph with PS and PMMA doped films.

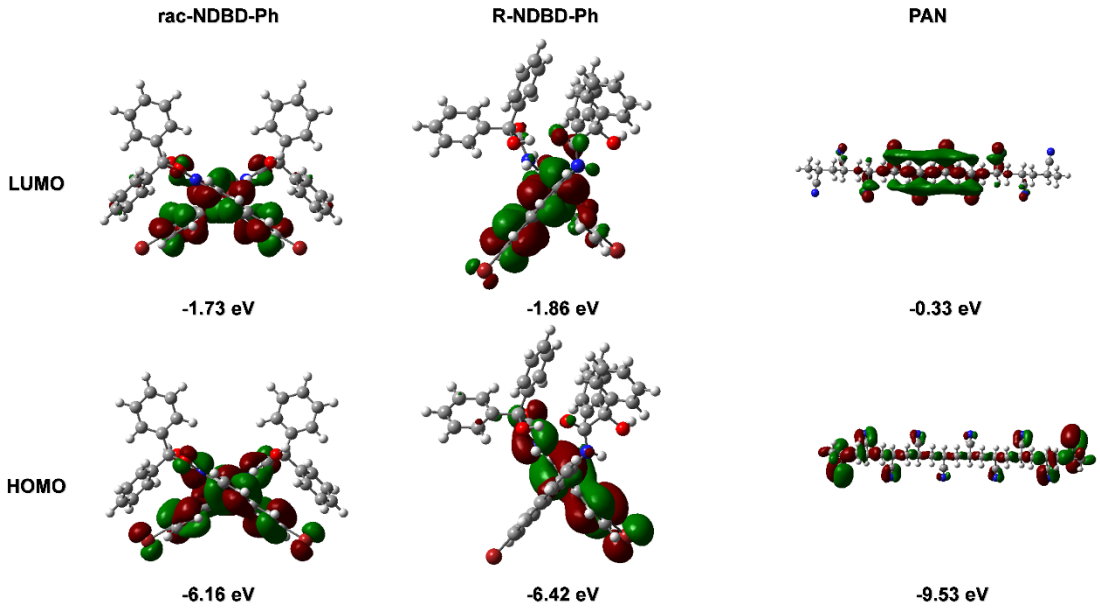

Figure S12. HOMO and LUMO distributions of rac-NDBD-Ph, R-NDBD-Ph and PAN.

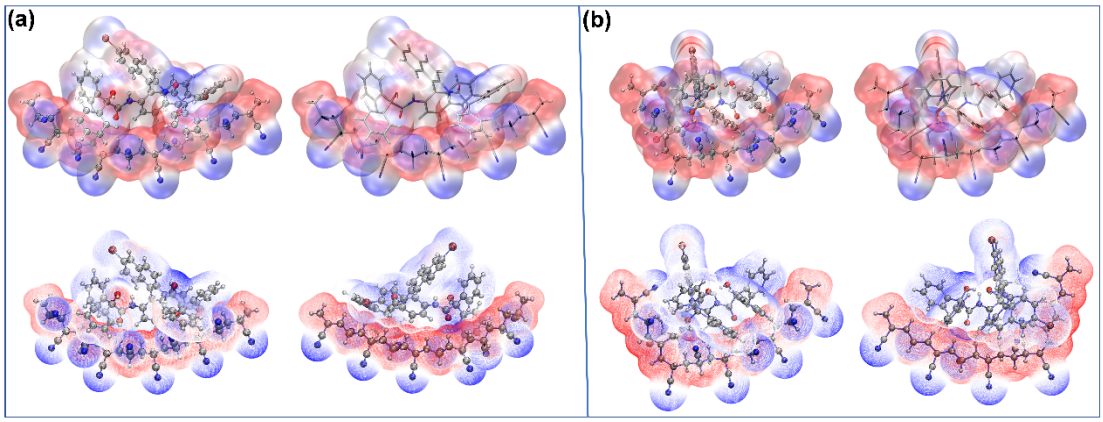

Figure S13. ESP surface of rac-NDBD-Ph@PAN and R-NDBD-Ph@PAN.

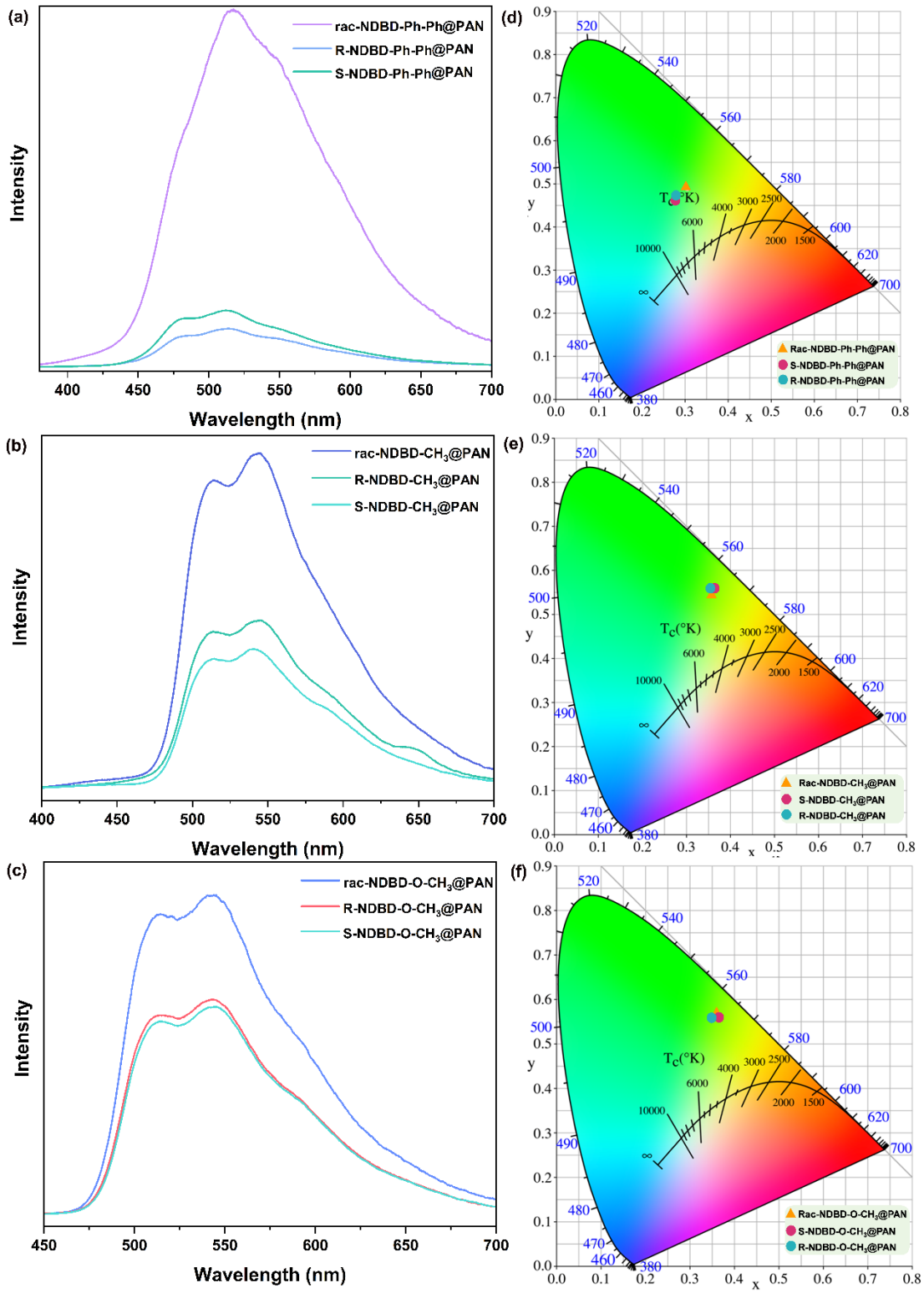

Figure S14. (a-c) Phosphorescence spectra and (d-f) the CIE 1931 coordinates of organic phosphors rac-NDBD-Ph-Ph, rac-NDBD-CH_3, rac-NDBD-O-CH_3 and R/S-NDBD-Ph-Ph, R/S-NDBD-CH_3, R/S-NDBD-O-CH_3 with PAN doped films.

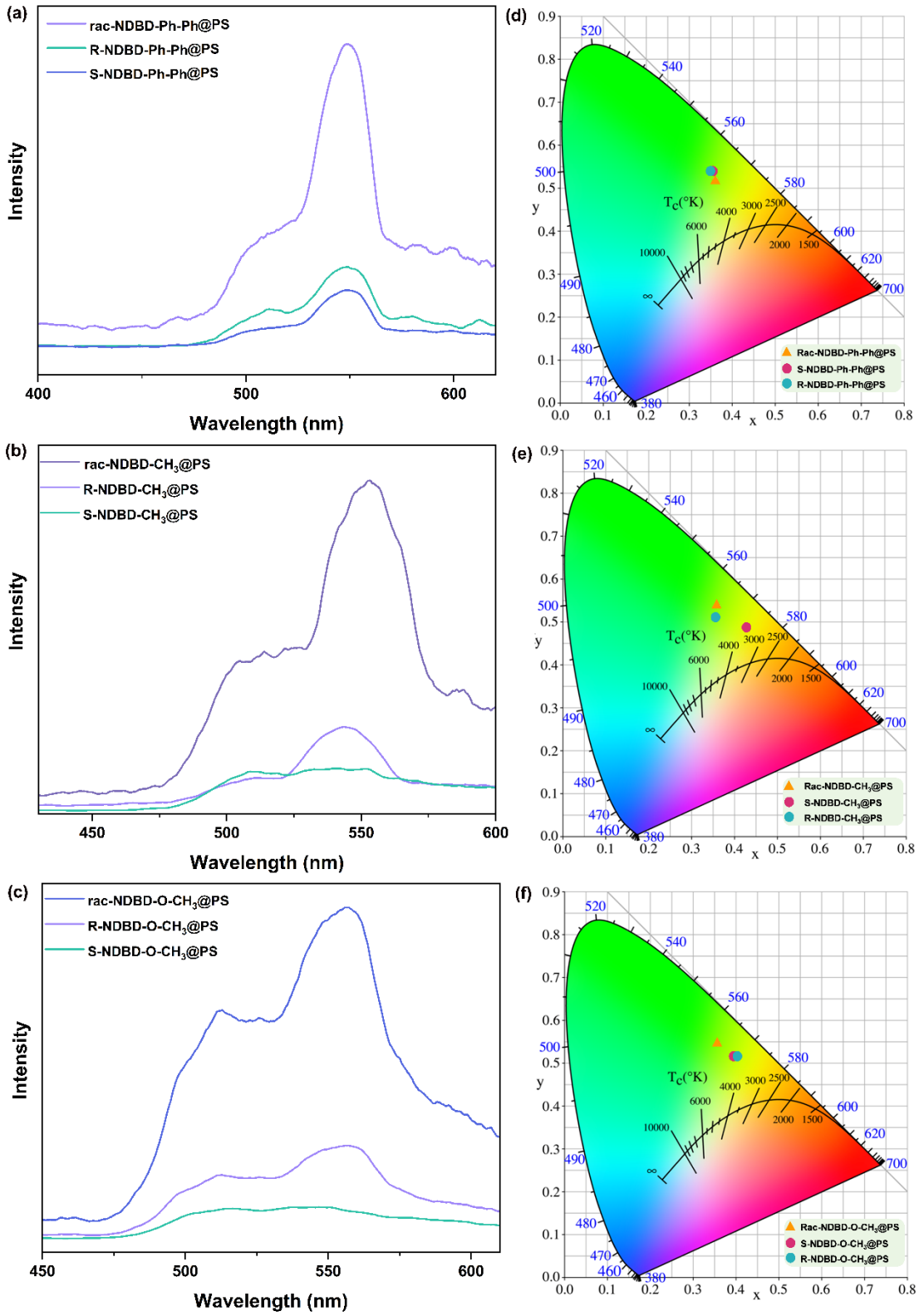

Figure S15. (a-c) Phosphorescence spectra and (d-f) the CIE 1931 coordinates of organic phosphors Rac-NDBD-Ph-Ph, Rac-NDBD-CH_3, Rac-NDBD-O-CH_3 and R/S-NDBD-Ph-Ph, R/S-NDBD-CH_3, R/S-NDBD-O-CH_3 with PS doped films.

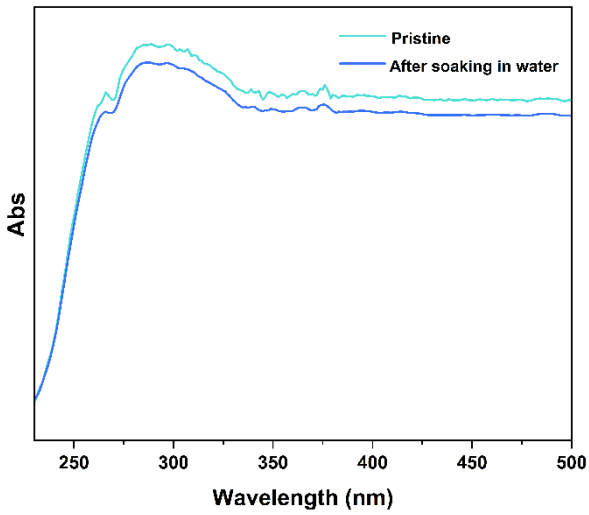

Figure S16. UV-vis absorption spectra of the rac-NDBD-Ph@PAN film in dry state and after soaking in water.

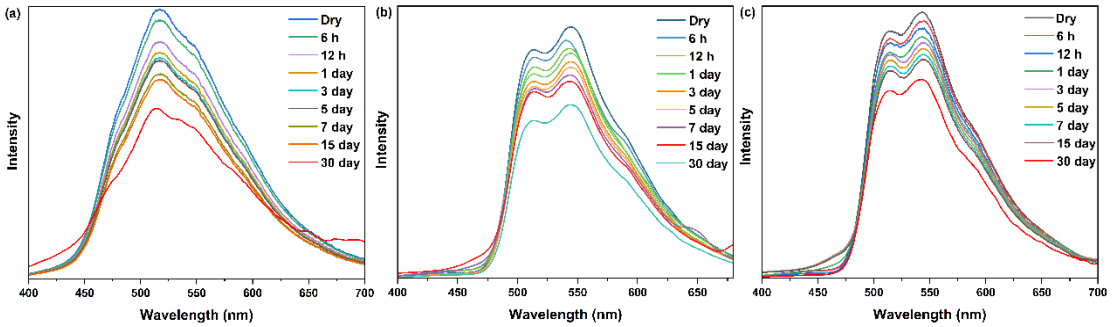

Figure S17. Delayed PL spectra recorded after the doped film (a) rac-NDBD-Ph-Ph@PAN, (b) rac-NDBD-CH_3@PAN and (c) rac-NDBD-O-CH_3@PAN was immersed in water for a certain time.

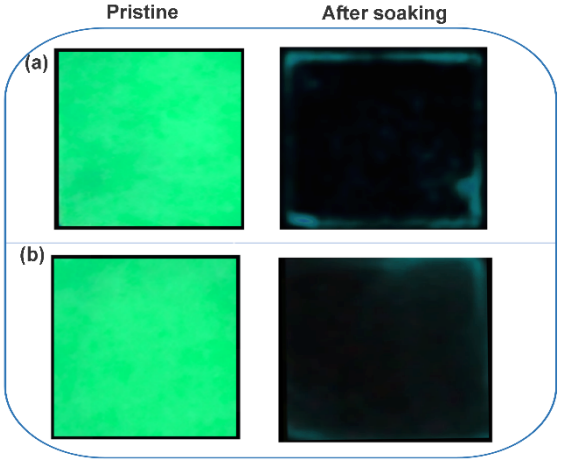

Figure S18. Afterglow Photographs of the doped films (a) R-NDBD-Ph@PAN and (b) S-NDBD-Ph@PAN in dry state and after soaking in water.

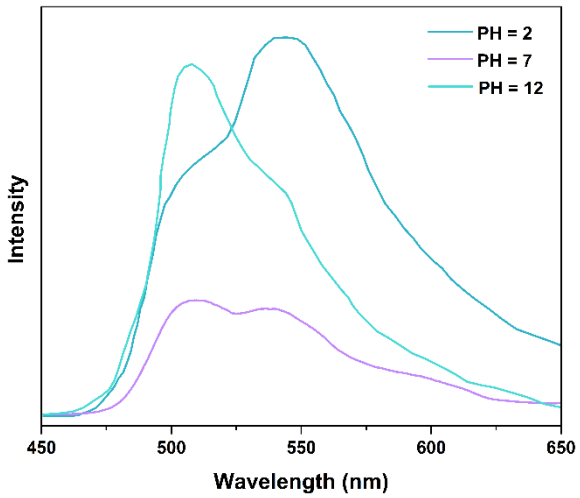

Figure S19. Delayed PL spectra of doped film rac-NDBD-Ph @PAN in different PH environments (delay: 2 ms).

Table S4. Structure data of R-NDBD-Ph-acid and R-NDBD-Ph-base single crystals.

Name	rac-NDBD-Ph-acid	r-NDBD-Ph-base
Formula	$C_{48}H_{34}Br_2N_2O_4$	$C_{96}H_{70}Br_4N_4O_{10}$
Temperature/K	297.74(18)	149.98(14)
Crystal system	monoclinic	triclinic
Space group	$C2_y$	P_1
Cell Lengths (Å)	a= 36.5216(6)	a=10.42669(14)
	b= 10.8114(2)	b=12.40814(15)
	c= 12.1409(2)	c= 18.05325(18)
Cell Angles (°)	α= 90	α= 79.3587(9)
	β= 97.5803(16)	β= 81.0124(10)
	γ= 90	γ=87.8419(10)
Cell Volume (Å^3)	4751.94(16)	2267.21(5)
Z	4	1
Density (g/cm^3)	1.206	1.288
F (000)	1752	894
Crystal size (mm^3)	0.15 × 0.13× 0.12	0.16 × 0.14× 0.12
Radiation	CuKα (λ = 1.54184)	CuKα (λ = 1.54184)
CCDC number	2336504	2336505

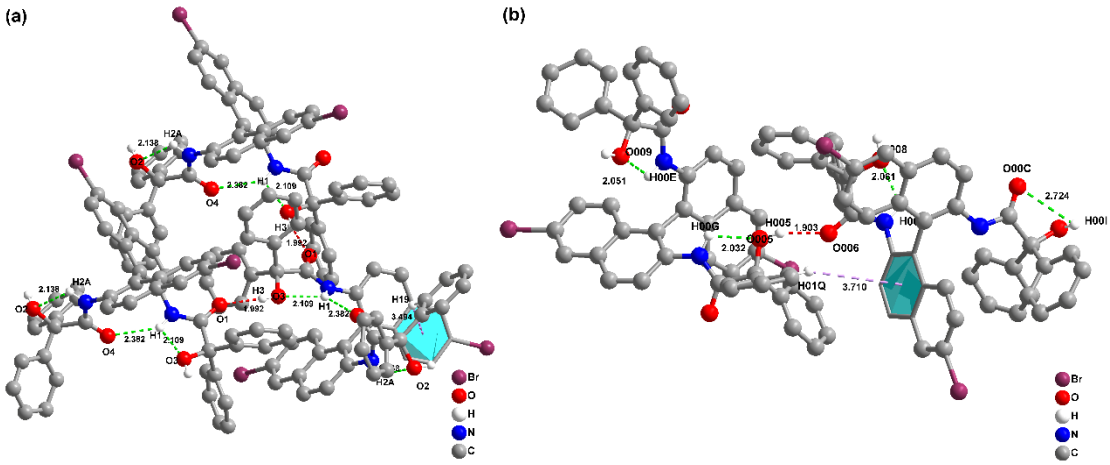

Figure S20. Intermolecular interactions of (a) R-NDBD-Ph-acid and (b) R-NDBD-Ph-base single molecules with neighboring molecules.

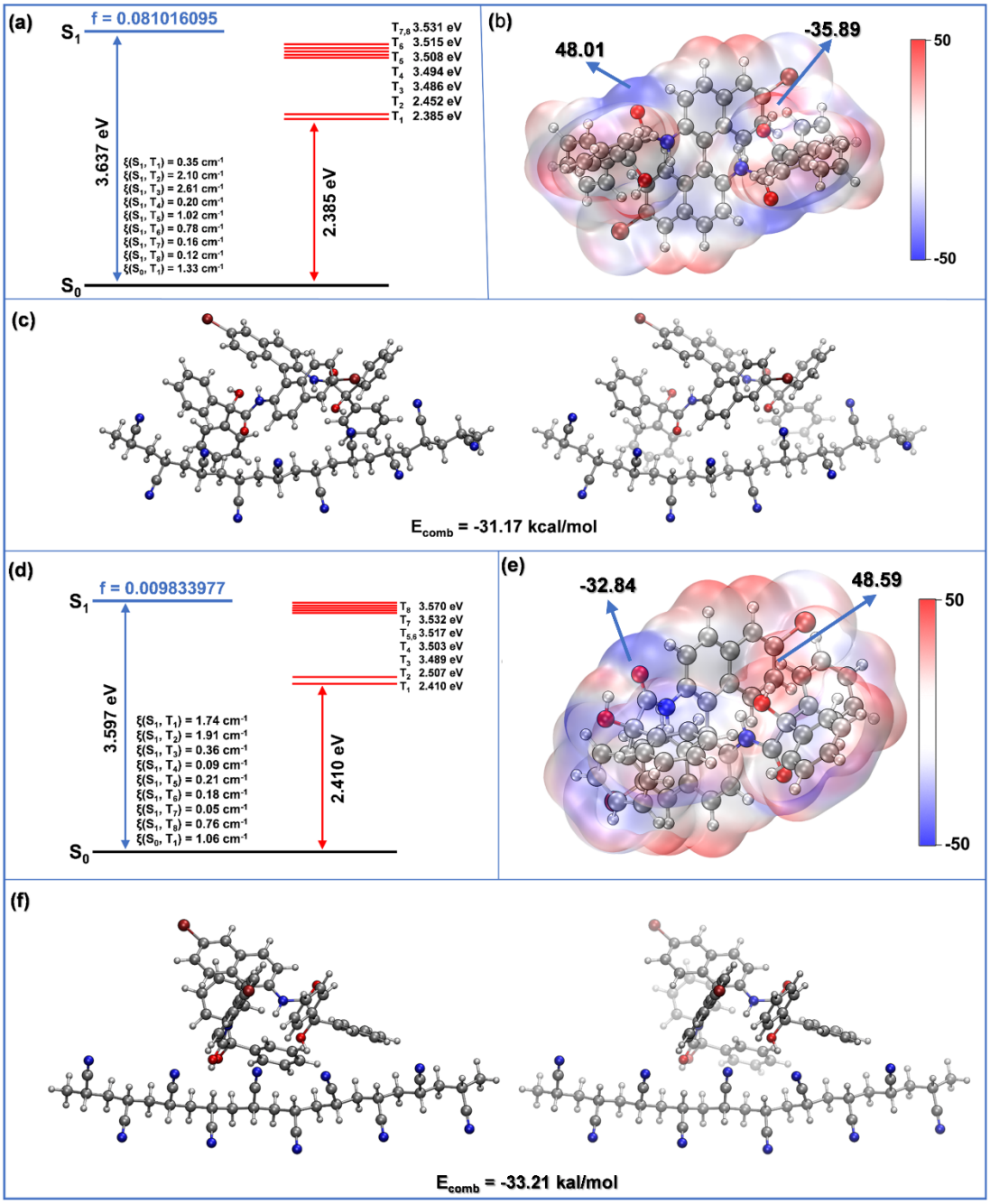

Figure S21. Mechanism of long-lived RTP of polymeric systems. Calculated SOC constant, calculated energy diagram and SOC (ξ) of small molecule (a) R-NDBD-Ph-acid and (d) R-NDBD-Ph-base. Molecular structures and calculated ESP distribution of (b) R-NDBD-Ph-acid and (e) R-NDBD-Ph-base. Calculated combining energy between organic phosphors (c) R-NDBD-Ph-acid, (f) R-NDBD-Ph-base and doped PAN matrix films.

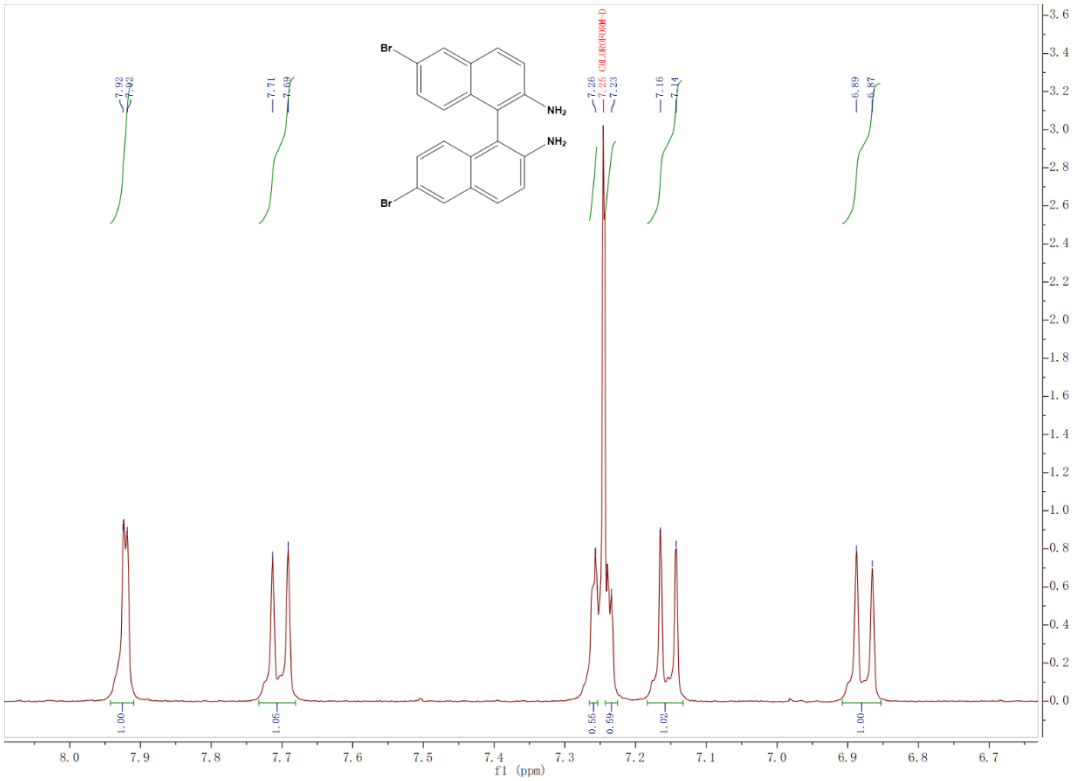

Figure S22. ^{1}H NMR spectrum of S-Br.

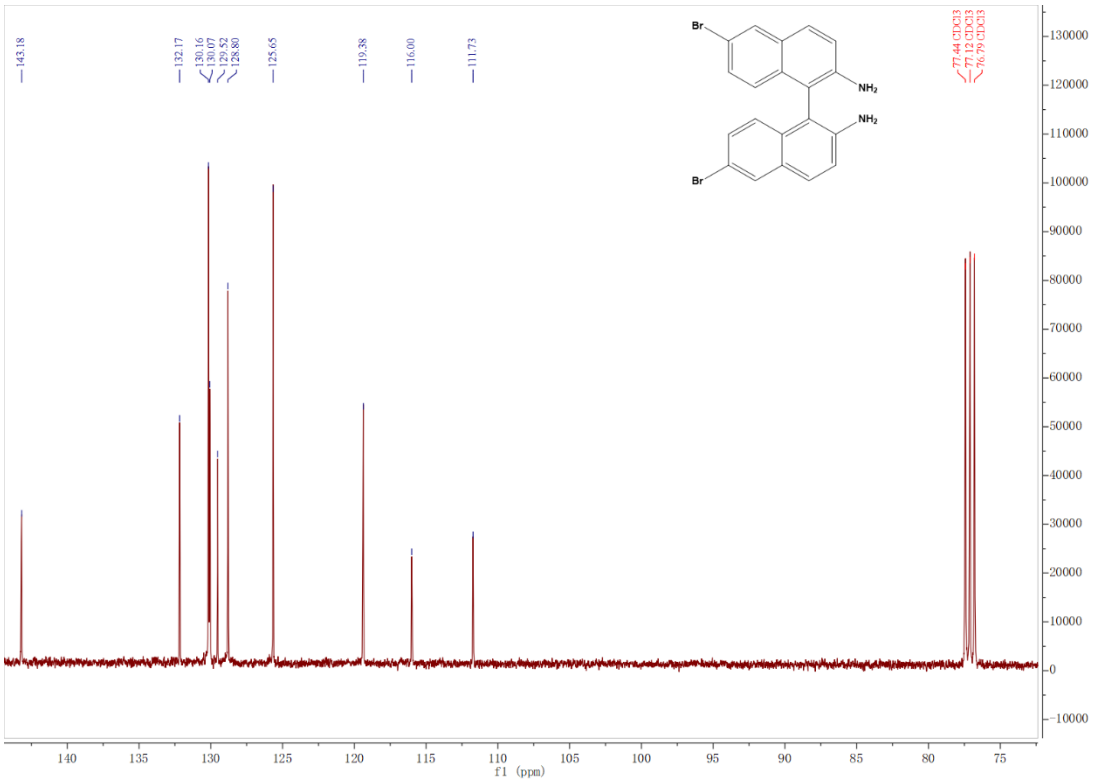

Figure S23. ^{13}C NMR spectrum of S-Br.

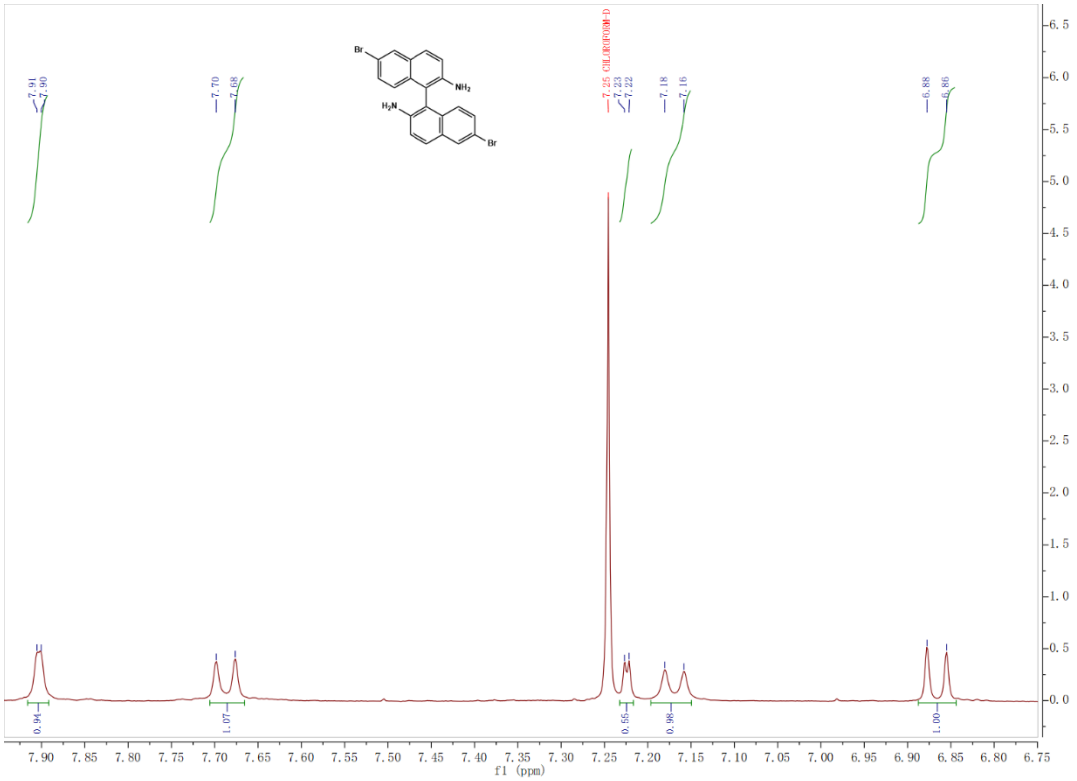

Figure S24. ^{1}H NMR spectrum of R-Br.

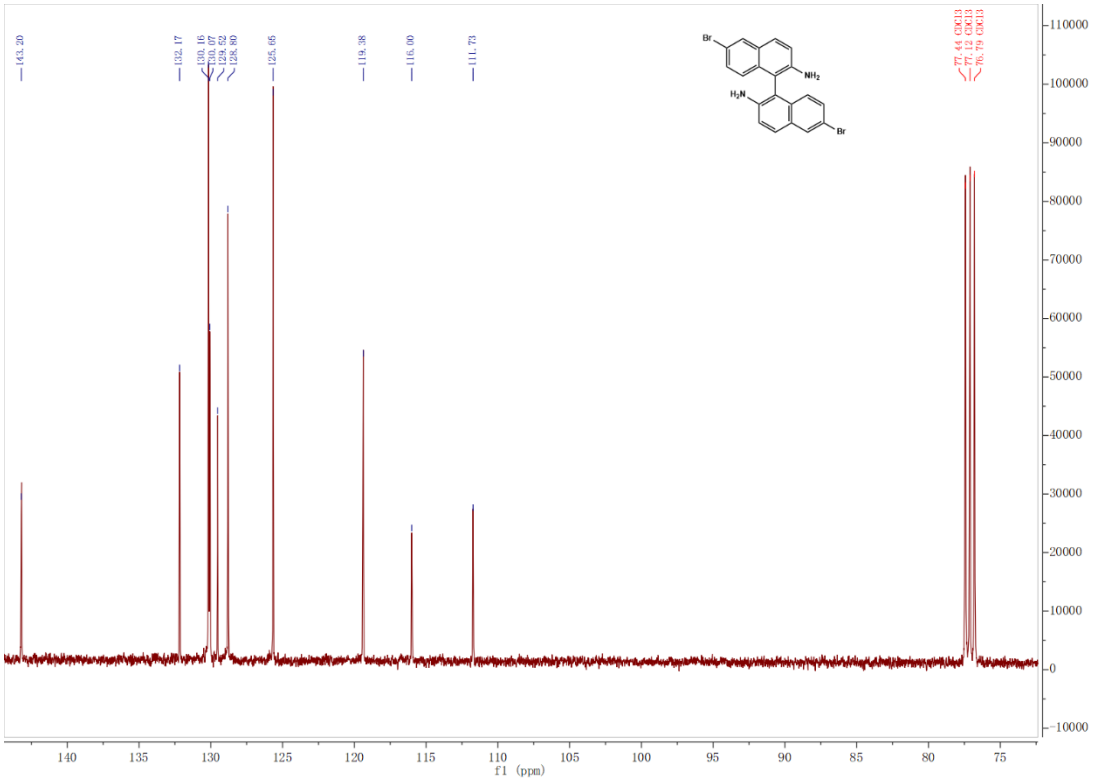

Figure S25. ^{13}C NMR spectrum of R-Br.

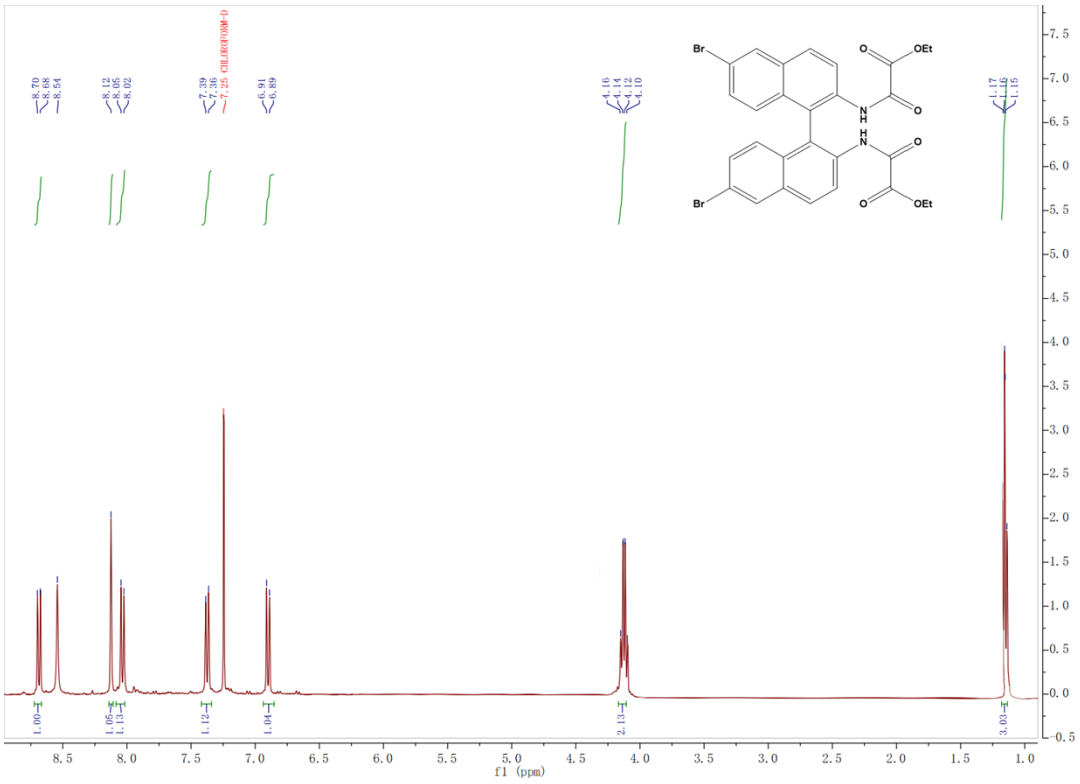

Figure S26. ^{1}H NMR spectrum of S-1.

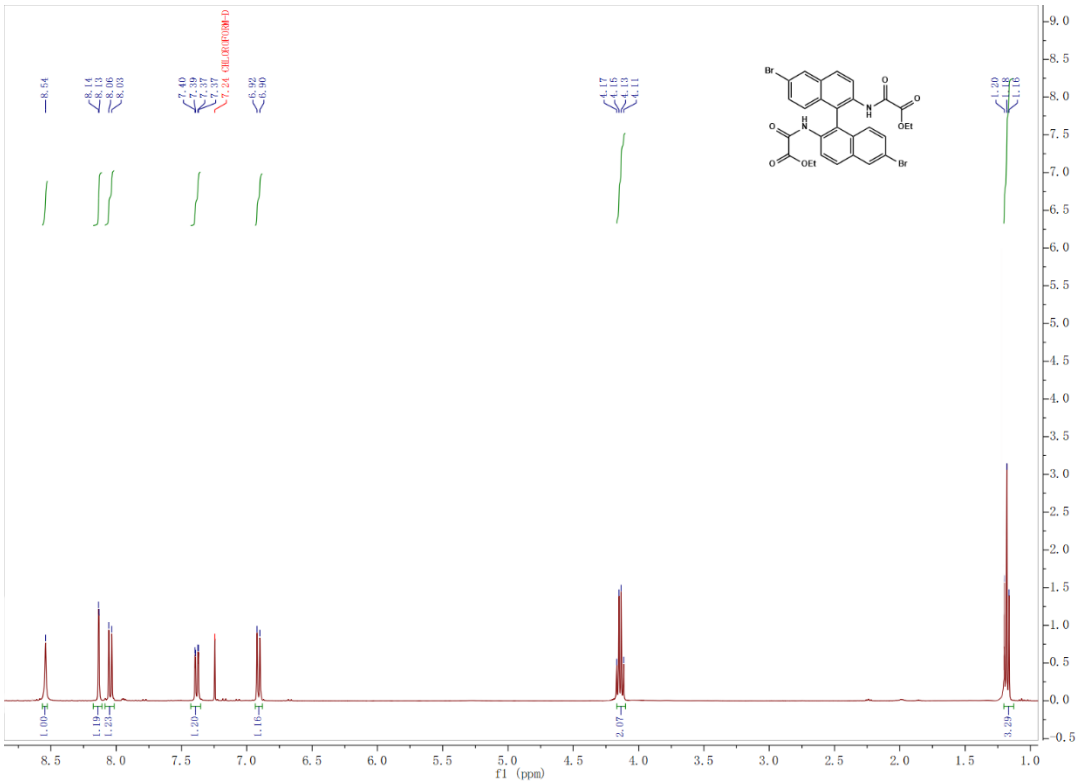

Figure S27. ^{1}H NMR spectrum of R-1.

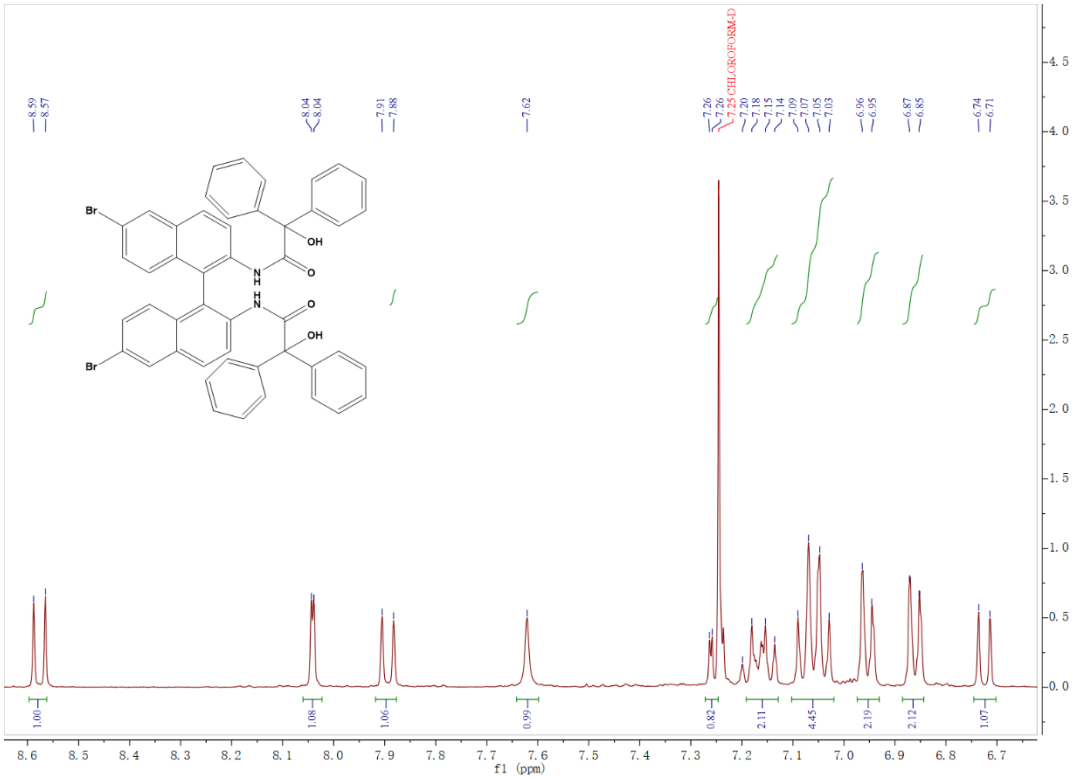

Figure S28. ^{1}H NMR spectrum of S-NDBD-Ph.

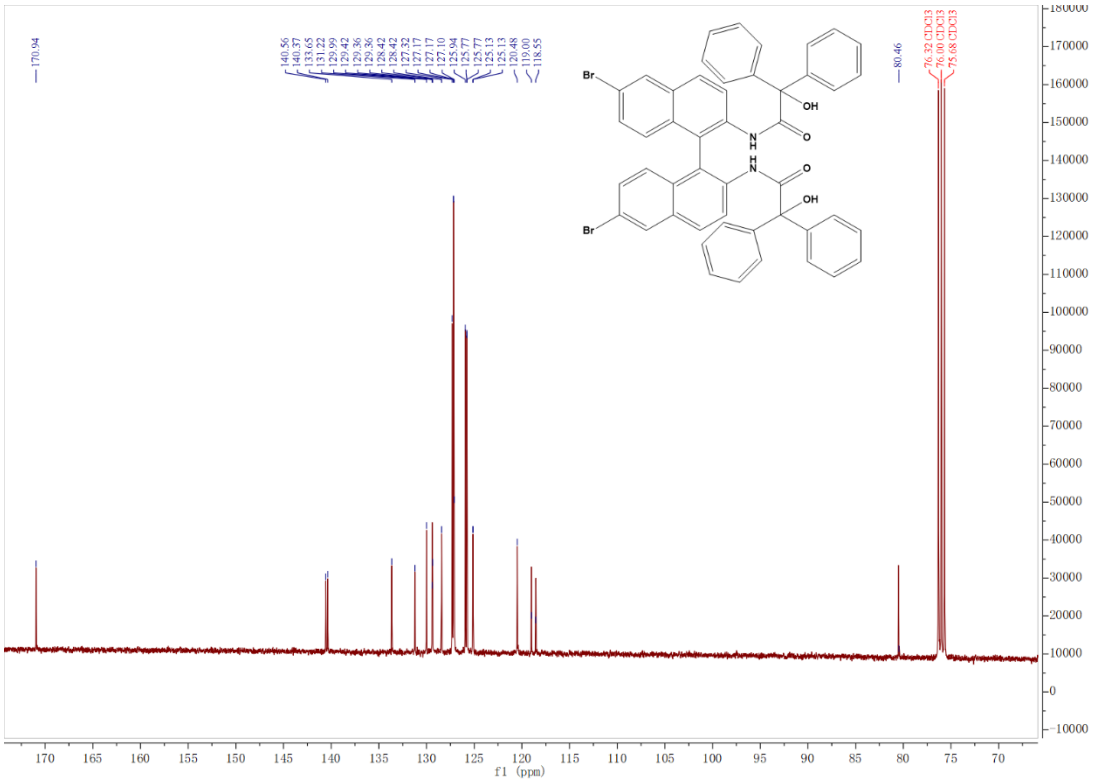

Figure S29. ^{13}C NMR spectrum of S-NDBD-Ph.

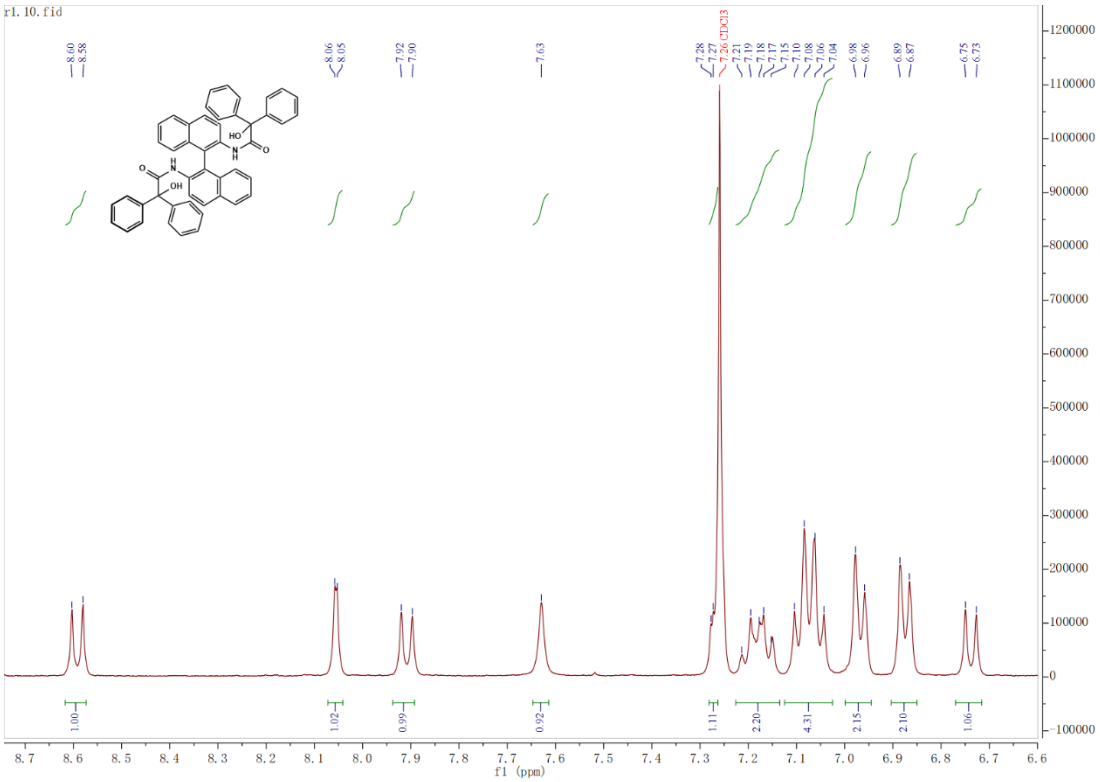

Figure S30. ^{1}H NMR spectrum of R-NDBD-Ph.

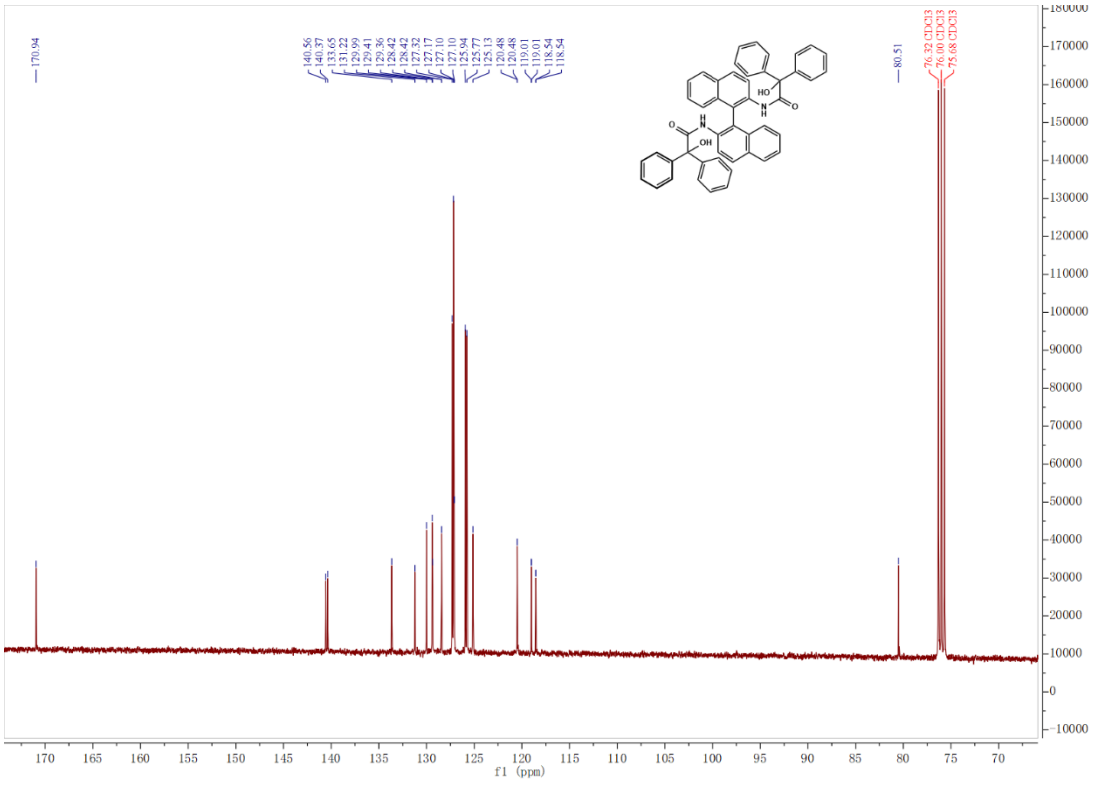

Figure S31. ^{13}C NMR spectrum of R-NDBD-Ph.

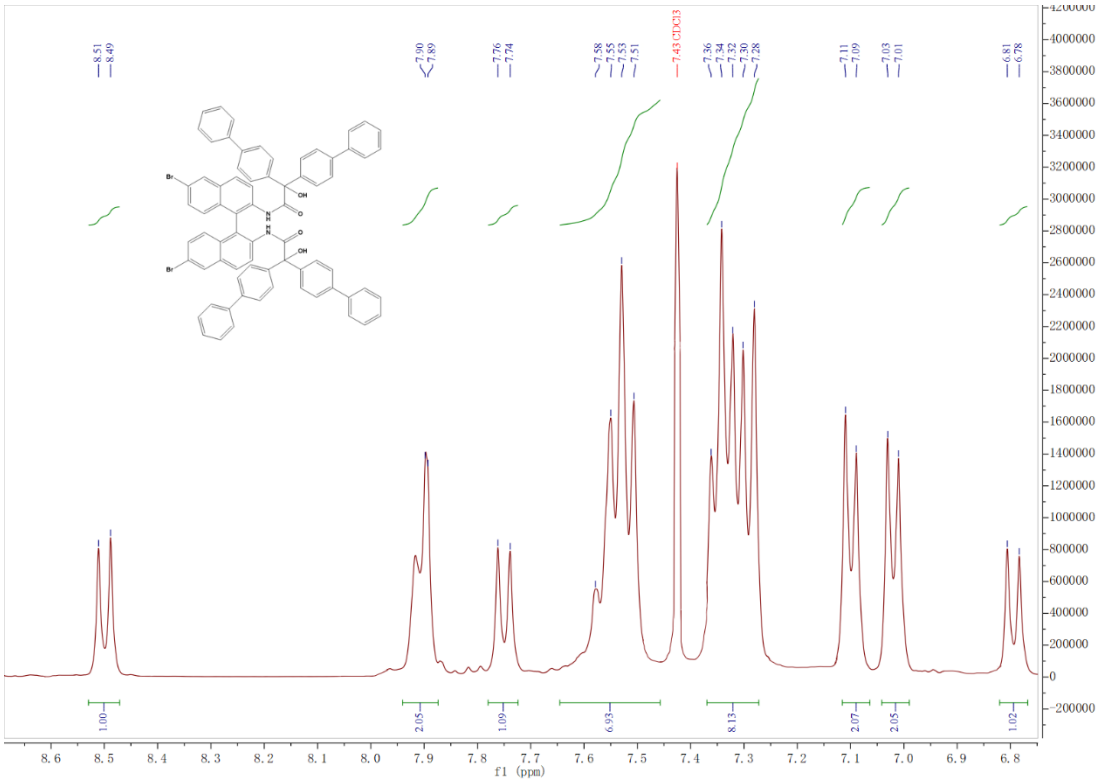

Figure S32. ^{1}H NMR spectrum of S-NDBD-Ph-Ph.

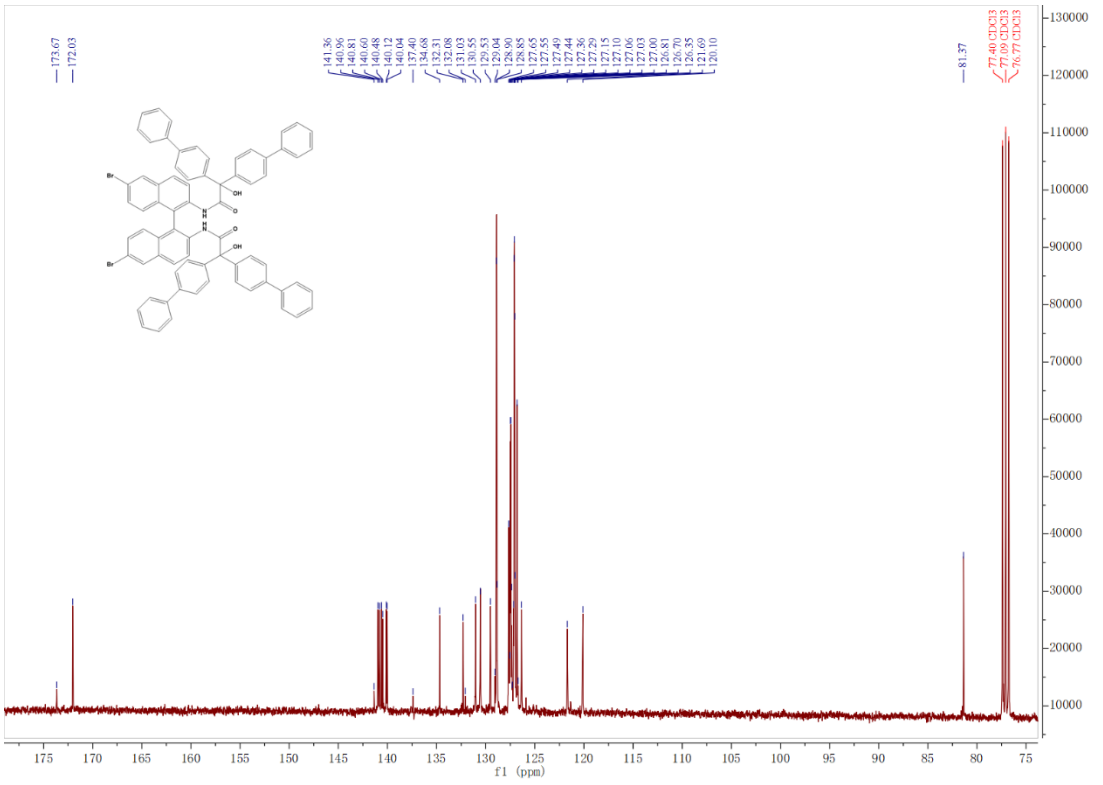

Figure S33. ^{13}C NMR spectrum of S-NDBD-Ph-Ph.

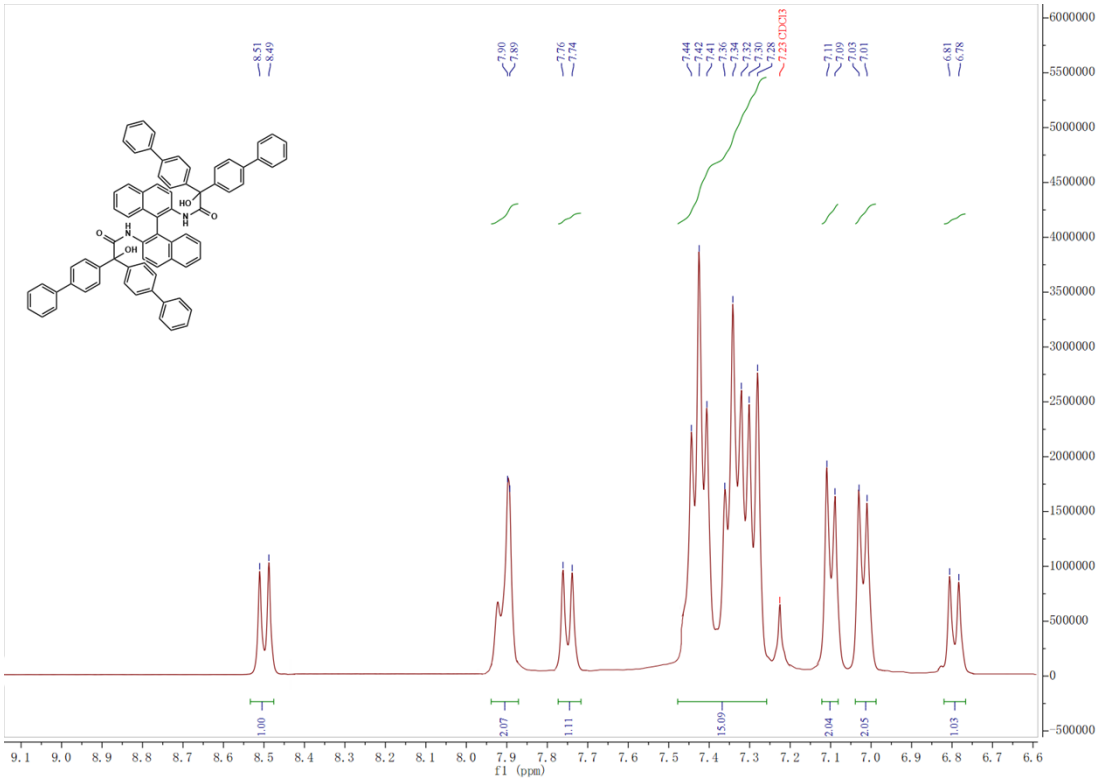

Figure S34. [1]H NMR spectrum of R-NDBD-Ph-Ph.

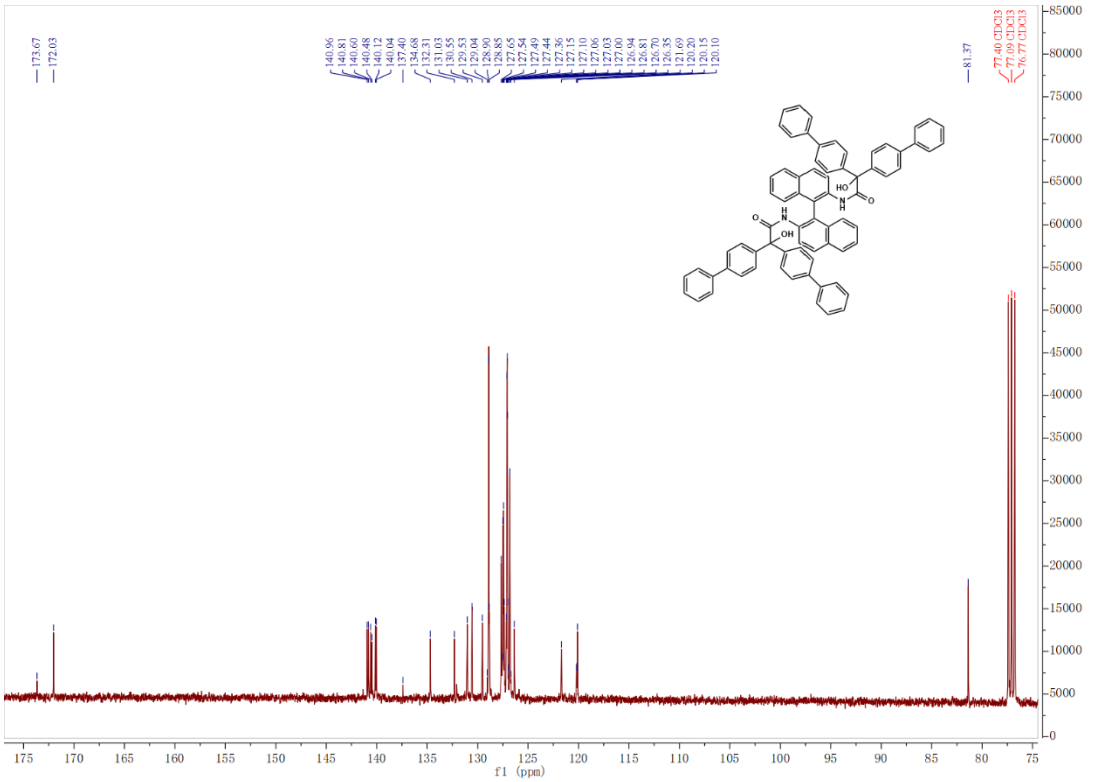

Figure S35. [13]C NMR spectrum of R-NDBD-Ph-Ph.

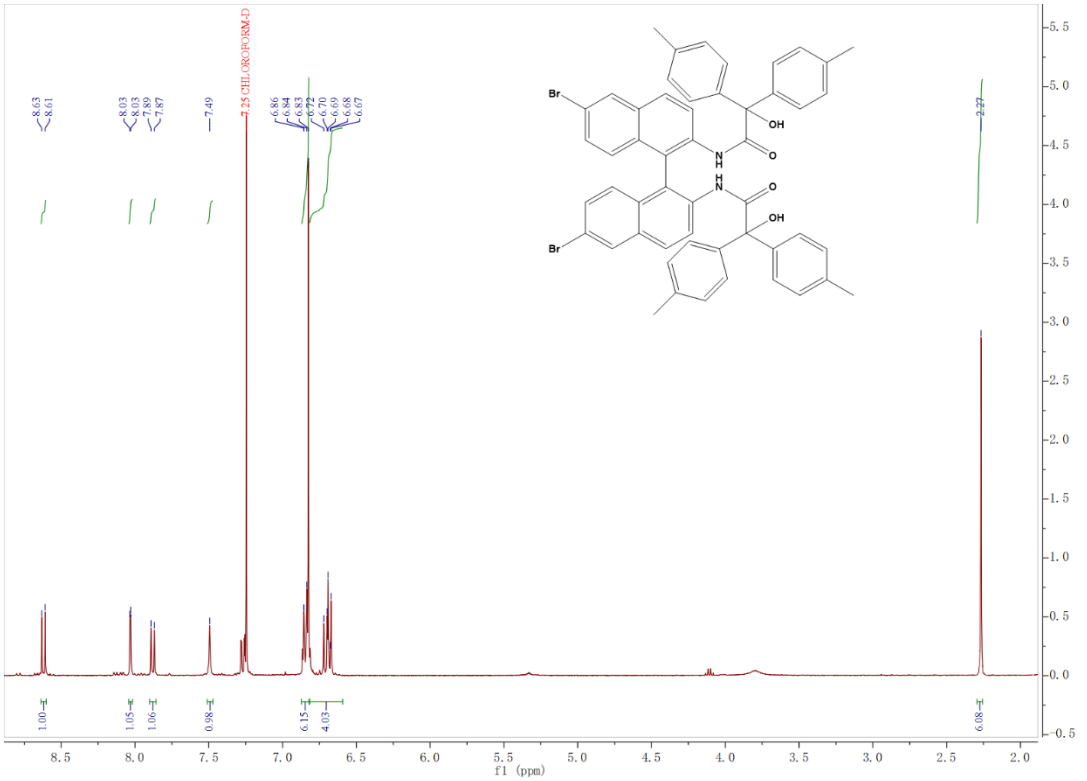

Figure S36. ^{1}H NMR spectrum of S-NDBD-CH_3.

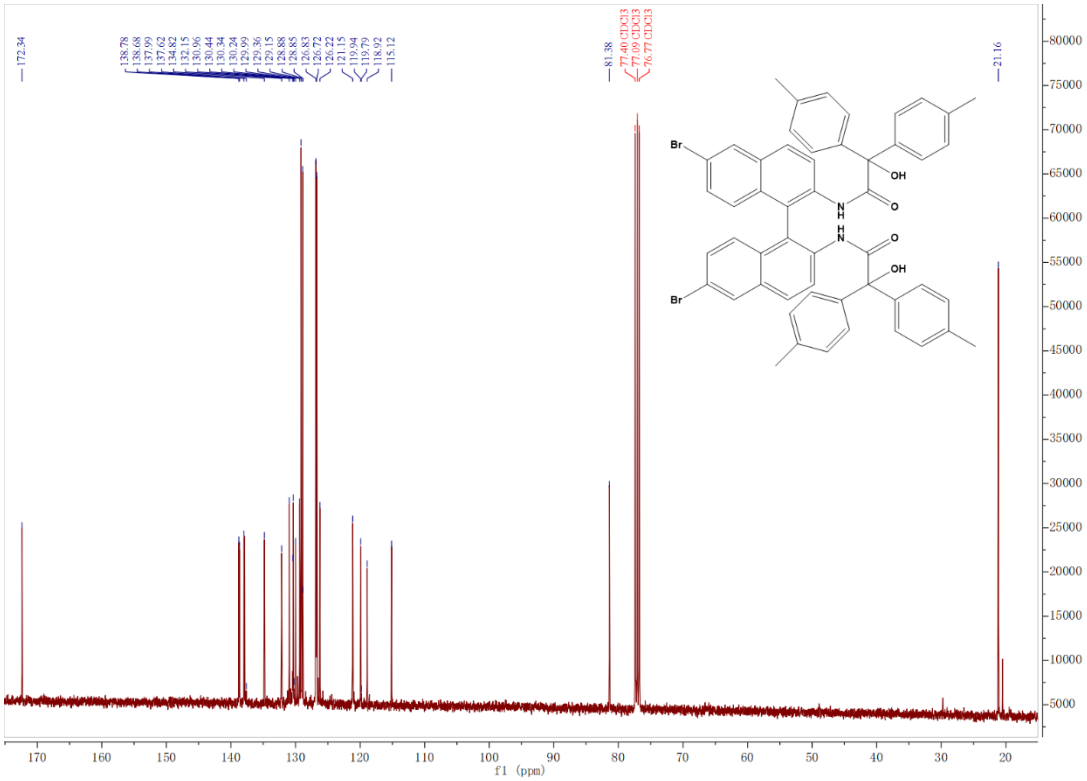

Figure S37. ^{13}C NMR spectrum of S-NDBD-CH_3.

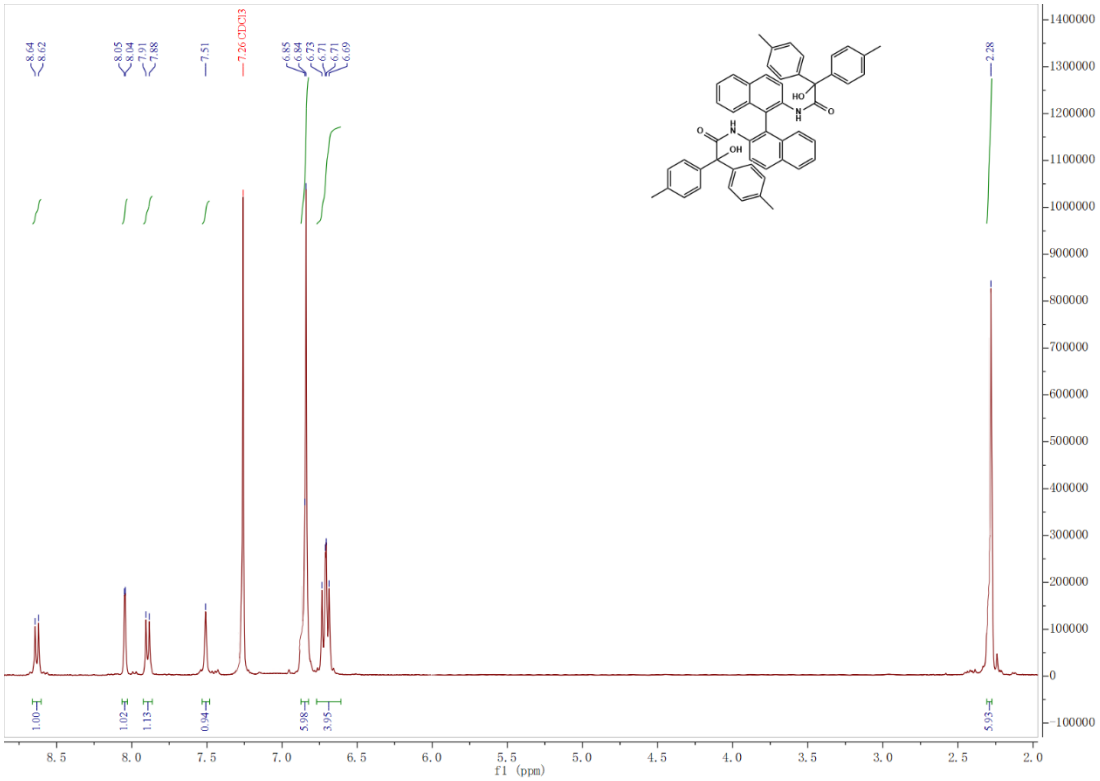

Figure S38. ^{1}H NMR spectrum of R-NDBD-CH$_3$.

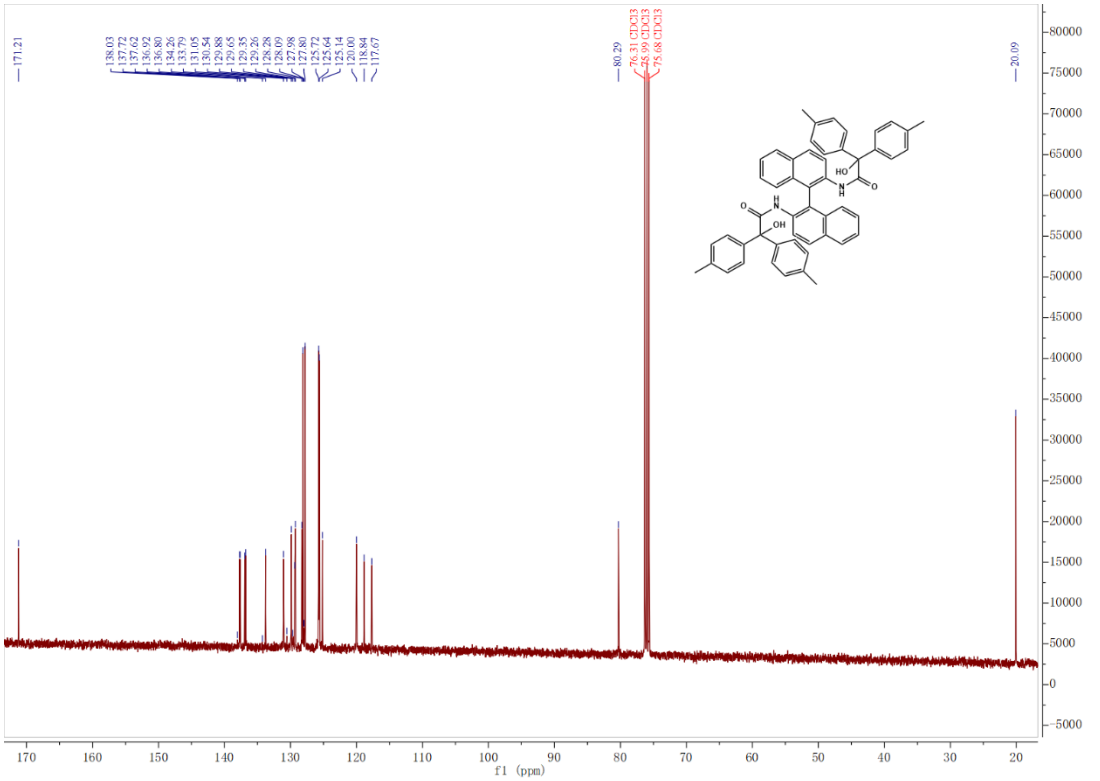

Figure S39. ^{13}C NMR spectrum of R-NDBD-CH$_3$.

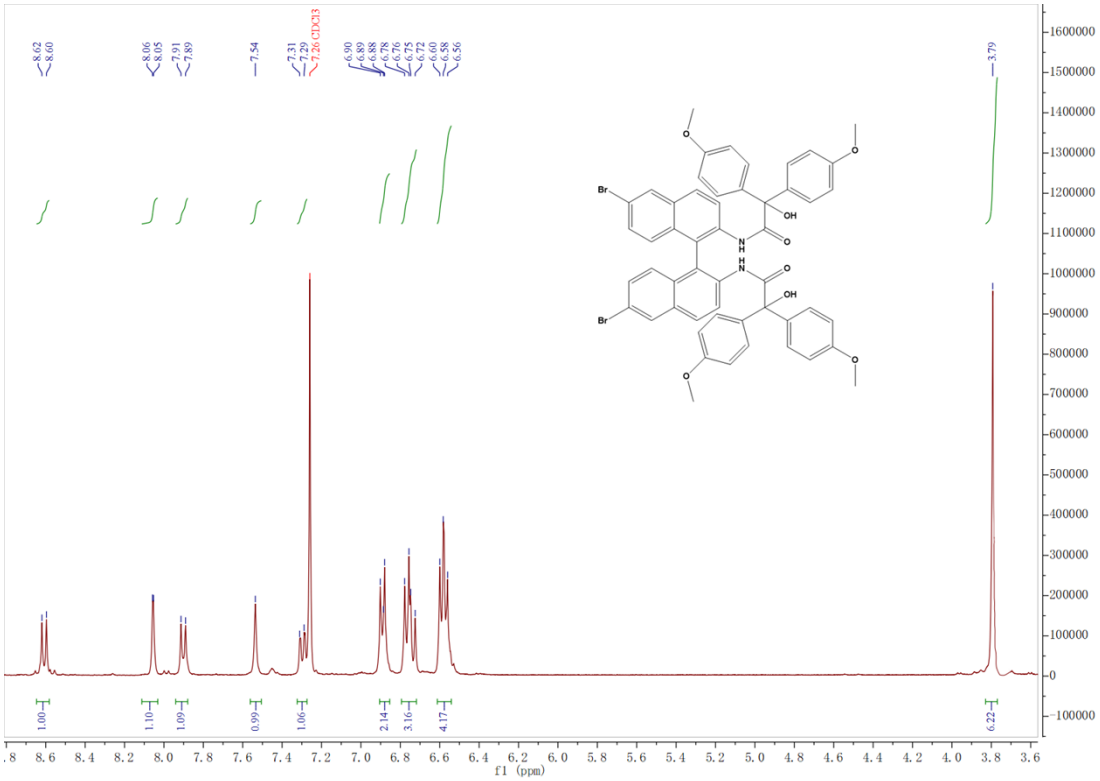

Figure S40. ^{1}H NMR spectrum of S-NDBD-O-CH_3.

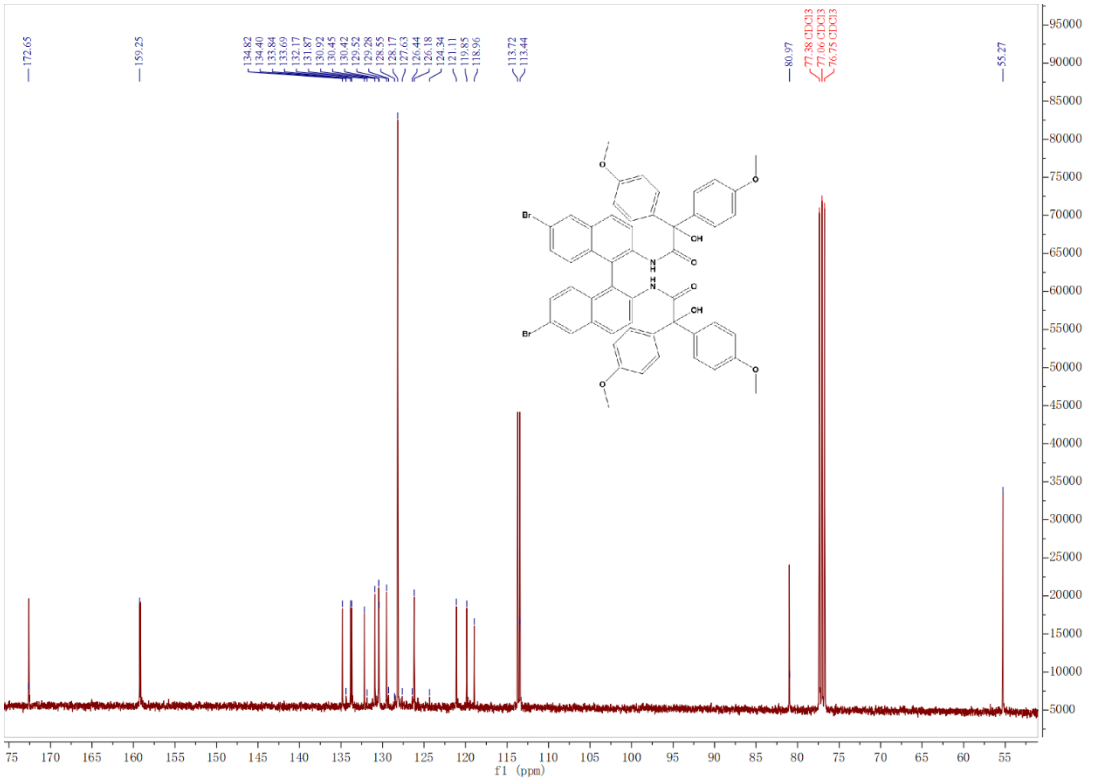

Figure S41. ^{13}C NMR spectrum of S-NDBD-O-CH_3.

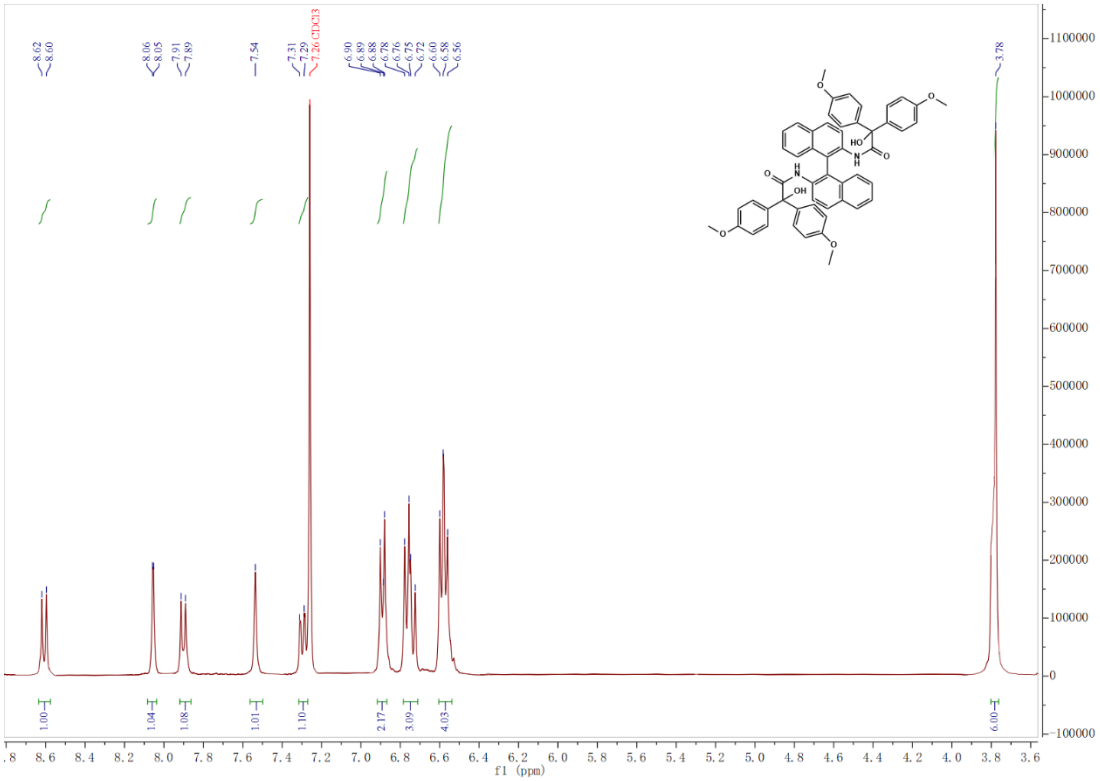

Figure S42. ^{1}H NMR spectrum of R-NDBD-O-CH$_3$.

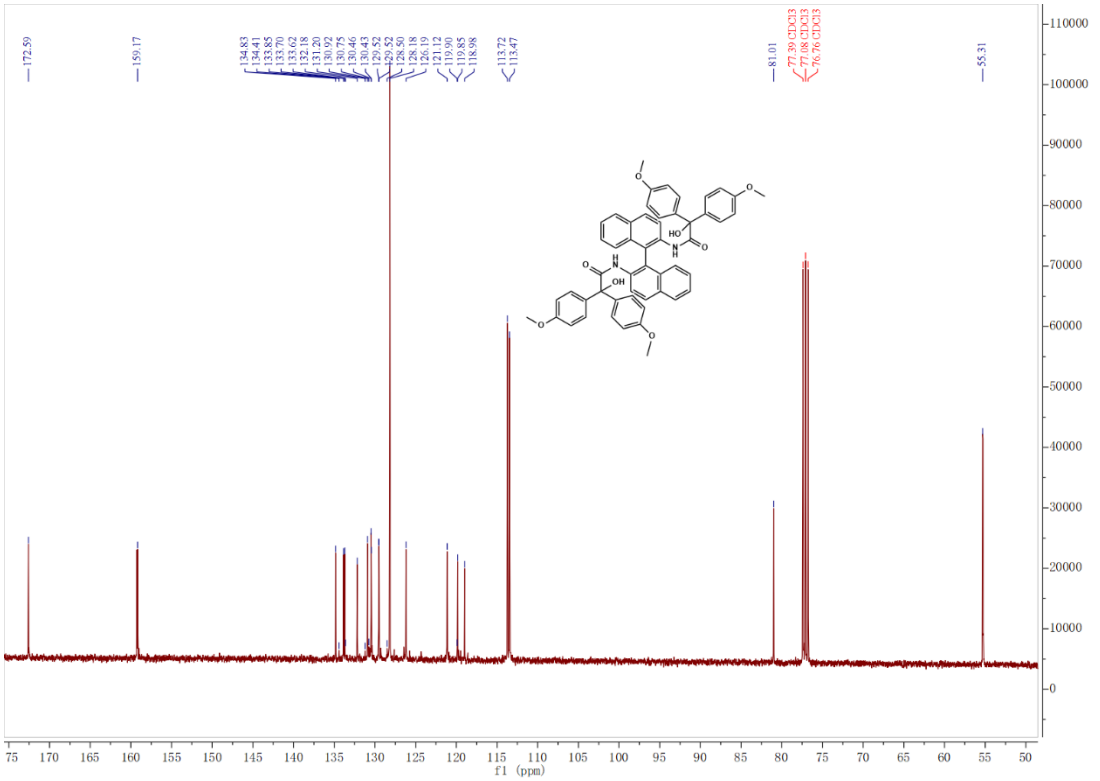

Figure S43. ^{13}C NMR spectrum of R-NDBD-O-CH$_3$.

REFERENCES

1 F. Neese, F. Wennmohs, U. Becker and C. Riplinger, *J. Chem. Phys.,* 2020, **152,** 224108.

2 L. Burns, Á. Mayagoitia, B. Sumpter and C. Sherrill, *J. Chem. Phys.,* 2011, **134,** 084107.

3 G. Stefan, *Chem. Eur. J.,* 2012, **18,** 9955.

4 T. Lu and F. Chen, *J. Comput. Chem.,* 2012, **33,** 580-592.

5 W. Humphrey, A. Dalke and K. Schulten, *J. Mol. Graph. Model.,* 1996, **14,** 33-38.

6 R. Gao, X. Y. Fang and D. P. Yan, *J. Mater. Chem. C,* 2018, **6,** 4444-4449.

7 R. Gao, D. P. Yan, D. G. Evans and X. Duan, *Nano Res.,* 2017, **10,** 3606-3617.

8 H. Z. Wu, D. L. Wang, Z. Zhao, D. Wang, Y. Xiong and B. Z. Tang, *Adv. Funct. Mater.*, 2021, **31,** 2101656.

9 X. X. Zheng, J. K. Jiang, Q. L. Lin, C. C. Li, J. S. Chen, S. W. Wang, Q. X. Han, X. Ye, Y. Liu and X. T. Tao, *Chem. Eng. J.,* 2023, **469,** 143929.

10 Y. F. Zhang, Y. Su, H. W. Wu, Z. H. Wang, C. Wang, Y. Zheng, X. Zheng, L. Gao, Q. Zhou, Y. Yang, X. H. Chen, C. L. Yang and Y. L. Zhao, *J. Am. Chem. Soc.,* 2021, **143,** 13675−13685.